frontiers | Frontiers in Endocrinology

TYPE Original Research
PUBLISHED 10 November 2022
DOI 10.3389/fendo.2022.1031013

OPEN ACCESS

EDITED BY
Reinaldo Marín,
Instituto Venezolano de Investigaciones Científicas (IVIC), Venezuela

REVIEWED BY
Xuntian Jiang,
Washington University in St. Louis, United States
Alison Ondrus,
California Institute of Technology, United States

*CORRESPONDENCE
William J. Griffiths
w.j.griffiths@swansea.ac.uk

SPECIALTY SECTION
This article was submitted to Developmental Endocrinology, a section of the journal Frontiers in Endocrinology

RECEIVED 29 August 2022
ACCEPTED 18 October 2022
PUBLISHED 10 November 2022

CITATION
Dickson AL, Yutuc E, Thornton CA, Wang Y and Griffiths WJ (2022) Identification of unusual oxysterols biosynthesised in human pregnancy by charge-tagging and liquid chromatography - mass spectrometry. *Front. Endocrinol.* 13:1031013. doi: 10.3389/fendo.2022.1031013

Identification of unusual oxysterols biosynthesised in human pregnancy by charge-tagging and liquid chromatography - mass spectrometry

Alison L. Dickson, Eylan Yutuc, Catherine A. Thornton, Yuqin Wang and William J. Griffiths*

Swansea University Medical School, Swansea, Wales, United Kingdom

The aim of this study was to identify oxysterols and any down-stream metabolites in placenta, umbilical cord blood plasma, maternal plasma and amniotic fluid to enhance our knowledge of the involvement of these molecules in pregnancy. We confirm the identification of 20S-hydroxycholesterol in human placenta, previously reported in a single publication, and propose a pathway from 22R-hydroxycholesterol to a C_{27} bile acid of probable structure 3β,20R,22R-trihydroxycholest-5-en-(25R)26-oic acid. The pathway is evident not only in placenta, but pathway intermediates are also found in umbilical cord plasma, maternal plasma and amniotic fluid but not non-pregnant women.

KEYWORDS

sterol, oxysterol, bile acids, CYP11A1, LC-MS, CYP27A1

1 Introduction

Amongst other functions, the placenta plays a key role in the transport of cholesterol from the mother to the fetus (1). The placenta is rich in cholesterol metabolising enzymes, particularly those involved in progesterone and estrogen synthesis (2). Hence, it should also be a site for oxysterol synthesis and further metabolism. Cytochrome P450 (CYP) 11A1 (also known as $P450_{SCC}$) is the enzyme that generates pregnenolone from cholesterol *via* consecutive 22R- and 20R-hydroxylations followed by side-chain cleavage (3). Progesterone is then formed from pregnenolone by oxidation at C-3 and Δ^5 – Δ^4 isomerisation by hydroxysteroid dehydrogenase (HSD) 3B1 (See Figure 1). Although 22R-hydroxycholesterol (22R-HC) and 20R,22R-dihydroxycholesterol (20R,22R-diHC)

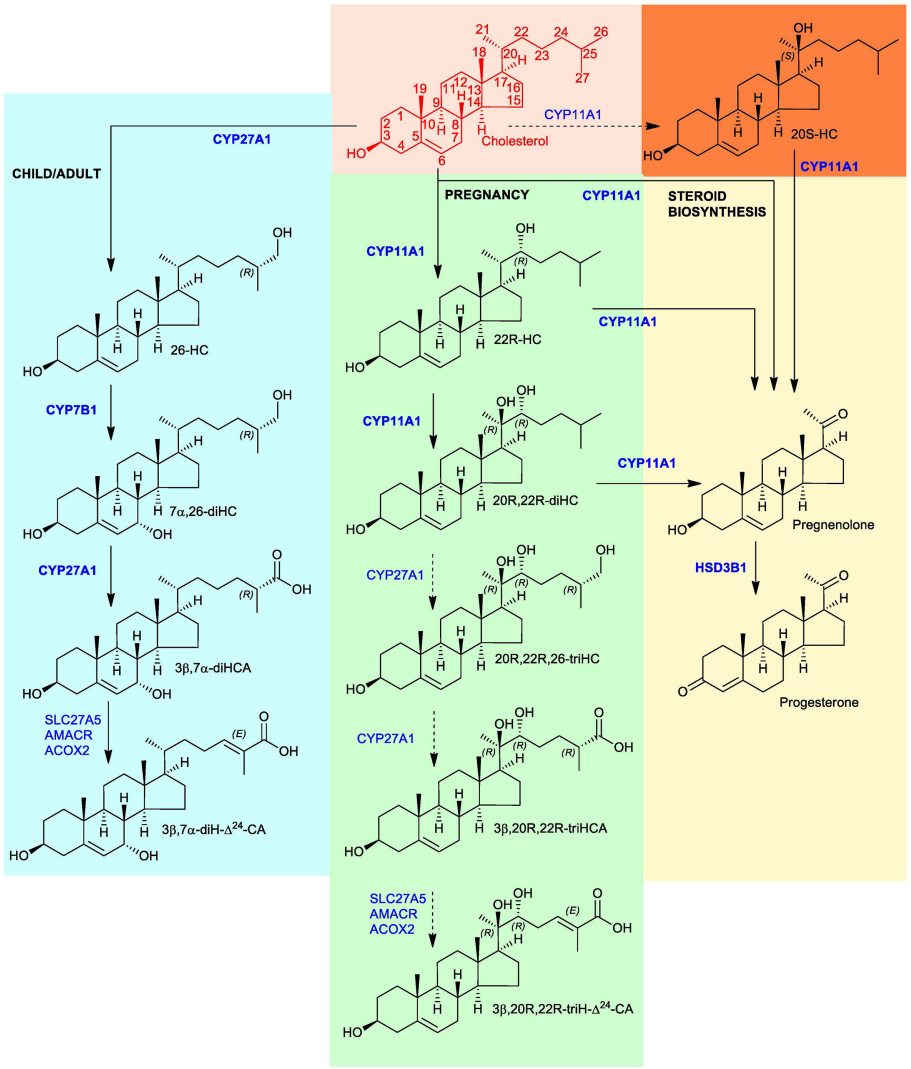

FIGURE 1
Proposed metabolism of cholesterol to the C_{27} bile acid 3β,20R,22R-triH-Δ^{24}-CA (green background). For comparison the acidic pathway to the C_{27} bile acid 3β,7α-diH-Δ^{24}-CA is shown (blue background) as is the pathway to progesterone (yellow background). Enzymes are indicated in blue. When shown in bold the enzymatic reactions can be found in the literature, when shown in normal typeface and with a broken arrow they are postulated. Cholesterol is shown in red with full stereochemistry and numbering system on a salmon background. For simplicity the 3β,20R,22R-triH-Δ^{24}-CA and 3β,7α-diH-Δ^{24}-CA are shown as the acids rather than the CoA-thioester products of SLC27A5 (bile acid CoA ligase). 20S-HC is shown on an orange background, although the enzyme responsible for its formation is unproven, it can be converted to 20R,22R-diHC by CYP11A1. Note the stereochemistry of metabolites down-stream of 20R,22R-diHC towards and including 3β,20R,22R-triH-Δ^{24}-CA are assumed based on biosynthetic considerations.

are known intermediates in CYP11A1-mediated side-chain cleavage of cholesterol to give pregnenolone (4), few studies have explored the oxysterol profile of placenta (5, 6). One important, but until now not replicated, finding made in the early 2000's was the presence of 20S-hydroxycholesterol (20S-HC) in human placenta (7). 20S-HC is an enigmatic oxysterol with many biological properties, but seldom reported in mammalian systems (8). Note, the actual stereochemical location of the 20S-hydroxy group in 20S-HC is the same as that of the 20R-hydroxy group in 20R,22R-diHC (see structures in Figure 1), but they are named 20S and 20R, respectively, according to rules of chemical priority. Similar to the situation with placenta, there are few reports of the oxysterol profiles of umbilical cord blood (5), i.e. blood of fetal origin that remains in the placenta and in the attached umbilical cord after childbirth, or of amniotic fluid, the fluid that acts as a cushion for the growing fetus and serves to facilitate the exchange of biochemicals between mother and fetus. Interestingly, however, oxysterols have been found as their sulphate esters in meconium, the earliest stool of a mammalian infant, including

20,22-diHC, 22-HC, 23-hydroxycholesterol (23-HC) and 24-hydroxycholesterol (24-HC) (9, 10).

Here we report liquid chromatography (LC) – mass spectrometry (MS)-based methods for the identification of oxysterols in full term placenta, plasma derived from cord blood and pregnant female blood (maternal blood) and in mid-gestation amniotic fluid. The methods are based on high mass resolution MS with multistage fragmentation (MS^n) exploiting charge-tagging to enhance analyte signal (Supplemental Figure S1A).

2 Materials and methods

2.1 Human material

Maternal blood was taken 24 - 48 hr prior to elective caesarean section at 37+ weeks of gestation for reasons that did not include maternal or fetal anomaly. Umbilical cord blood was collected at delivery of the baby. Control plasma was from non-pregnant females. Amniotic fluid was obtained at 16 – 18 weeks of pregnancy during diagnostic amniocentesis; only samples with no fetal chromosomal abnormality were used. All samples were collected with approval from an appropriate Health Research Authority Research Ethics Committee. All participants provided informed consent and the study adhered to the principles of the Declaration of Helsinki.

2.2 Sterol and oxysterol standards

Isotope-labelled standards [25,26,26,26,27,27,27-$^2H_7$]24R/S-hydroxycholesterol ([$^2H_7$]24R/S-HC), [25,26,26,26,27,27,27-$^2H_7$]22R-hydroxycholesterol ([$^2H_7$]22R-HC), [25,26,26,26,27,27,27-$^2H_7$]22S-hydroxycholesterol ([$^2H_7$]22S-HC), [25,26,26,26,27,27,27-$^2H_7$]7α-hydroxycholesterol ([$^2H_7$]7α-HC), [26,26,26,27,27,27-$^2H_6$]7α,25-dihydroxycholesterol ([$^2H_6$]7α,25-diHC) were from Avanti Polar Lipids, Alabaster, AL. [25,26,26,26,27,27,27-$^2H_7$]20S-Hydroxycholesterol ([$^2H_7$]20S-HC) was purchased from Toronto Research Chemicals (TCI, Toronto, Canada). [$^2H_7$]22R-Hydroxycholest-4-en-3-one ([$^2H_7$]22R-HCO) was prepared from [$^2H_7$]22R-HC by treatment with cholesterol oxidase enzyme (*Streptomyces* sp., Merck, Dorset, UK) (11).

2.3 Sterol and oxysterol extraction

2.3.1 Placenta

Sterols and oxysterols were extracted from placental tissue using a modified protocol previously used to extract oxysterols from brain and liver tissue (12, 13). Approximately 400 mg of tissue was cut from the maternal side of fresh placenta, weighed and washed three times in PBS to remove blood. The tissue was then transferred to a gentleMACS™ C tube (Miltenyi Biotec, Woking, UK) followed by 4.2 mL of absolute ethanol containing 50 ng of [$^2H_7$]24R/S-HC and 50 ng of [$^2H_7$]22R-HCO. The tissue was homogenised for 2 min. The homogenate was transferred to a 15 mL corning tube and sonicated for 15 min. Whilst sonicating, 1.8 mL of HPLC grade water was added dropwise to give 6 mL of homogenate at 70% ethanol. The homogenate was then centrifuged for 1 hr at 4,000 x *g*. The supernatant was transferred to a fresh 15 mL corning tube and the remaining pellet re-suspended in a further 4.2 mL ethanol containing 50 ng of [$^2H_7$]24R/S-HC and 50 ng of [$^2H_7$]22R-HCO. The suspension was vortex mixed and transferred back into the original gentleMACS™ C tube where it was then homogenised for a further 2 min. The homogenate was removed and sonicated for 15 min, then 1.8 mL of water added to give 6 mL of 70% ethanol. The supernatants from the two extractions were combined to yield 12 mL in 70% ethanol. This was mixed by vortex and sonicated for a further 10 min followed by centrifugation for 1 hr at 4,000 x *g*. Ten % (1.2 mL) of the total supernatant was added to 300 µL of 70% ethanol under sonication. The 1.5 mL of sample was subjected to solid phase extraction (SPE) by a procedure modified from an earlier protocol (12, 13) to allow the collection of C_{21} steroids besides sterols and oxysterols including sterol acids.

The sample from above was loaded onto a Certified Sep-Pak C_{18}, 200 mg (3 cm^3, Waters Inc. Elstree, UK) reversed-phase SPE column previously conditioned with ethanol (4 mL) followed by 70% ethanol (6 mL). The sample flow-through (1.5 mL) was combined with a column wash of 70% ethanol (5.5 mL) resulting in SPE1-Fr1 (7 mL) which contained oxysterols, sterol acids and C_{21} steroids. A second fraction was obtained by further washing with 70% ethanol (4 mL) and collected as SPE1-Fr2. Cholesterol and other sterols of similar hydrophobicity were eluted from the SPE column with absolute ethanol (2 mL) to give SPE1-Fr3. A final fourth fraction was eluted with a further 2 mL of absolute ethanol (SPE1-Fr4). Each of the four fractions was divided equally into A and B sub-fractions and dried overnight under vacuum by centrifugal evaporation (ScanLaf ScanSpeed vacuum concentrator, Lynge, Denmark).

Each lyophilised sample was reconstituted in propan-2-ol (100 µL) and mixed thoroughly by vortex. To fractions (A), 50 mM K_2HPO_4 buffer, pH 7 (1 mL) containing cholesterol oxidase solution (3.0 µL, 2 mg/mL in water, 44 units/mg of protein) was added. The samples were mixed by vortex and incubated at 37°C for 1 hr in a water bath. The reaction was then quenched by the addition of methanol (2 mL). Fractions (B) were treated in parallel in an identical fashion to fractions (A) but in the absence of cholesterol oxidase. Glacial acetic acid (150 µL) was added to fractions (A) and (B) and mixed by vortex. [$^2H_5$]Girard P (GP) reagent (11) (190 mg, bromide salt) was added to fractions (A) and [$^2H_0$]GP reagent (150 mg, chloride salt, TCI Europe, Oxford UK) was added to fractions (B). The samples were mixed by vortex until the derivatising reagent had dissolved. The reaction

was left to proceed overnight at room temperature protected from light.

An OASIS HLB 60 mg (3 cm^3) SPE cartridge was washed with methanol (6 mL), 5% methanol (6 mL) and conditioned with 70% methanol (4 mL). Sample from above (3.25 mL, 69% organic) was loaded onto the column and the flow-through collected. The sample tube was rinsed with 70% methanol (1 mL) which was then loaded onto the SPE column, and the eluent combined with the earlier flow-through. The column was re-conditioned with 35% methanol (1 mL) and the eluent combined with the earlier collection. The total eluent (~5 mL) was diluted with 4 mL of water to give ~9 mL of 35% methanol. The 9 mL sample solution was loaded onto the column and the flow-through collected. The sorbent was re-conditioned with 17.5% methanol (1 mL) and the eluent combined with earlier flow-through. To the combined 10 mL, water (9 mL) was added to give a 19 mL of 17.5% methanol. This solution was loaded onto the column and the flow-through collected once more. The sorbent was re-conditioned with 8.75% methanol (1 mL) and the flow-through combined with the earlier collection. The total combined eluent of 20 mL was diluted with 19 mL of water to give 39 mL 8.75% methanol. The solution was loaded onto the column and the flow-through discarded. A 5% methanol solution (6 mL) was used to wash the column before the analytes were eluted. The samples were eluted into four separate 1.5 mL microcentrifuge tubes using 3 x 1 mL methanol followed by 1 mL ethanol to give SPE2-FR1, -Fr2, -Fr3, -Fr4. Oxysterols originating from SPE1-Fr1 elute across SPE2-Fr1 and SPE2-Fr2, cholesterol originating from SPE1-Fr3 elutes across SPE2-Fr1,-Fr2, Fr-3. Here we report data only for oxysterols and more polar metabolites.

Immediately prior to LC-MS analysis of oxysterols, equal volumes of SPE2-Fr1A and SPE2-Fr2A were combined with equal aliquots of SPE2-Fr1B and SPE2-Fr2B and diluted with water to form a solvent composition of 60% methanol.

2.3.2 Plasma

The extraction protocol for sterols and oxysterols was essentially that described previously (11, 13, 14), with minor modification to allow for extraction of C_{21} steroids. 100 µL of plasma was added dropwise to a solution of acetonitrile (1.05 mL) containing 20 ng of [$^2H_7$]24R/S-HC and 20 ng of [$^2H_7$]22R-HCO in an ultrasonic bath with sonication. After a further 5 min of sonication, 350 µL of water was added. The sample (1.5 mL), now in 70% acetonitrile, was sonicated for a further 5 minutes and centrifuged at 17,000 x *g* at 4°C for 30 min. The sample was subjected to SPE and prepared for LC-MS analysis exactly as for the placental extract with the following modification: SPE1, Certified Sep-Pak C_{18}, 200 mg, was conditioned with 70% acetonitrile rather than 70% ethanol.

2.3.3 Amniotic fluid

The protocol for extraction of sterols and oxysterols from amniotic fluid was exactly as that described for plasma except the internal standards were 7 ng of [$^2H_7$]24R/S-HC and 7 ng of [$^2H_7$]22R-HCO.

2.4 LC-MS(MS^n)

Analysis was performed on a Dionex Ultimate 3000 UHPLC system (Dionex, now Thermo Fisher Scientific, Hemel Hempstead, UK) interfaced *via* an electrospray ionisation (ESI) probe to an Orbitrap Elite MS (Thermo Fisher Scientific). Chromatographic separation was carried out on a Hypersil Gold reversed phase C_{18} column (1.9 µm particle size, 50 x 2.1 mm, Thermo Fisher Scientific, UK). Details of the mobile phase and gradients employed are given in Supplemental Materials and Methods. MS analysis on the Orbitrap Elite was performed in the positive-ion mode with five scan events, one high resolution (120,000 full width at half maximum height at *m/z* 400) scan over the *m/z* range 400 – 610 in the Orbitrap and four MS^3 scans performed in parallel in the linear ion trap (LIT). Mass accuracy in the Orbitrap was typically < 5 ppm. More details of the scan events are provided in Supplemental Materials and Methods. Injection volumes were 35 µL for plasma extracts and at 90 µL for amniotic fluid and placental extracts.

3 Results

The aim of this study was to identify oxysterols and any downstream metabolites in placenta, cord plasma, maternal plasma and amniotic fluid to enhance our knowledge of the involvement of these molecules in pregnancy. For side-chain oxysterols expected to be present quantitative measurements were possible by reference to an isotope-labelled standard, for unexpected metabolites only semi-quantitative data was obtained, however, this could be used for relative quantification between sample sets (Table 1).

3.1 Identification of oxysterols in placenta

The placenta is a blood-rich organ. The maternal side contains less vascular tissue than the fetal side and was selected for analysis. During sample preparation tissue was washed three times with PBS to remove blood.

3.1.1 Monohydroxycholesterols:- 20S-HC, 22R-HC, 22S-HC, 24S-HC, 26-HC, 7α-HC and 7β-HC

Shown in Figure 2A (upper panel) is the LC-MS reconstructed ion chromatogram (RIC) for monohydroxycholesterols (HC, *m/z* 539.4368 ± 5ppm) found in placenta following derivatisation with [$^2H_5$]GP reagent. At first glance, the chromatogram shows some similarity to that of adult plasma (Figure 2A central panel) except

TABLE 1 Oxysterols in placenta, cord plasma, maternal plasma and amniotic fluid.

m/z	Compound	Placenta[1]	Cord Plasma	Maternal Plasma	Control Female Plasma	Amniotic Fluid	Quantification	Characteristic ion
$[^2H_5]$GP or $[^2H_0]$GP	Abbreviation	ng/g (SD) n=3	ng/mL (SD) n=14	ng/mL (SD) n=10	ng/mL (SD) n=5	ng/mL (SD) n=5		
539.4368	**7α-HC**	D/NM	31.46 (32.45)	57.27 (35.00)	46.08 (39.70)[2]	D/NM	Semi-quantitative[3]	151 (*b_1-12), 231 (*c_2-H_2O+2H)
534.4054	**7α-HCO**	D/NM	0.65 (0.74)	12.51 (9.34)	1.33 (2.97)[2]	D/NM	Semi-quantitative[3]	151 (*b_1-12), 231 (*c_2-H_2O+2H)
539.4368	**7β-HC**	D/NM	33.87 (38.68)	77.26 (61.09)	70.77 (74.37)[2]	D/NM	Semi-quantitative[3]	151 (*b_1-12), 231 (*c_2-H_2O+2H)
539.4368	**20S-HC**	D/NM	ND	ND	ND	ND	Not quantified[4]	151 (*b_1-12), 163 (*b_3-28), 327 (*e')
539.4368	**22R-HC**	210.3 (16.1)	6.19 (3.01)	2.55 (1.18)	ND	0.31 (0.34)	Quantitative[5]	151 (*b_1-12), 163 (*b_3-28), 273 (*d_1-12), 353 ('*f), 355 (*f')
539.4368	**22S-HC**	D/NM	ND	ND	ND	ND	Not quantified	151 (*b_1-12), 163 (*b_3-28), 273 (*d_1-12), 353 ('*f), 355 (*f')
539.4368	**24S-HC**	D/NM	7.34 (2.38)	14.99 (4.28)	14.48 (3.33)	D/NM	Quantitative[5]	151 (*b_1-12), 163 (*b_3-28), 353 ('*f)
539.4368	**26-HC**	41.5 (3.20)	7.23 (2.88)	21.61 (5.63)	25.67 (2.30)	D/NM	Quantitative[5]	151 (*b_1-12), 163 (*b_3-28), 427 (M-Py-CO) > 437 (M-Py-H_2O)
555.4317	**7α,26-diHC**	D/NM[6]	0.49 (0.23)	1.03 (0.54)	1.08 (0.55)	0.04 (0.03)	Semi-quantitative[3]	151 (*b_1-12), 231 (*c_2-H_2O+2H), 410 (M-Py-H_2O-CO-NH)
550.4003	**7α,26-diHCO**	D/NM[6]	3.24 (1.26)	3.89 (1.19)	4.13 (1.23)	0.19 (0.13)	Semi-quantitative[3]	151 (*b_1-12), 231 (*c_2-H_2O+2H), 410 (M-Py-H_2O-CO-NH)
555.4317	**20R,22R-diHC**	D/NM	49.74 (23.97)	13.23 (6.79)	ND	3.02 (1.63)	Quantitative[5]	151 (*b_1-12), 163 (*b_3-28), 325 ('*e), 327 (*e'), 353 ('*f-16), 355 (*f'-16)
555.4317	**22,23-diHC** [7]	D/NM	ND	ND	ND	ND	Semi-quatitative[7]	151 (*b_1-12), 163 (*b_3-28), 327 (*e'), 353 ('*f), 367 ('*g-16)
571.4266	**20R,22R,23-triHC** [7]	D/NM	D/NM	ND	ND	ND	Not quantified	151 (*b_1-12), 163 (*b_3-28), 325 ('*e), 327 (*e'), 353 ('*f-16), 355 (*f'-16), 383 ('*g-16)
571.4266	**20R,22R,24-triHC** [7]	D/NM	D/NM	ND	ND	ND	Not quantified	151 (*b_1-12), 163 (*b_3-28), 325 ('*e), 327 (*e'), 353 ('*f-16), 383 ('*g-16), 397 ('*h-16)
571.4266	**20R,22R,26-triHC** [7]	D/NM	0.30 (0.23)	0.06 (0.06)	ND	0.04 (0.03)	Semi-quantitative[7,8]	151 (*b_1-12), 163 (*b_3-28), 325 ('*e), 327 (*e'), 353 ('*f-16), 355 (*f'-16)
553.4161	**3β-HCA**	4.14 (0.48)	10.56 (4.71)	43.64 (13.71)	90.02 (21.40)	0.73 (0.46)	Quantitative[5]	151 (*b_1-12), 163 (*b_3-28), 423 ('*j), 426 (M-Py-CO-NH)
583.3902	**3β,20R,22R-triH-Δ^{24}-CA** [7]	D/NM	D/NM	ND	ND	D/NM	Not quantified	151 (*b_1-12), 163 (*b_3-28), 325 ('*e), 327 (*e'), 353 ('*f-16), 369 ('*f), 371 (*f'), 417 ('*j-36), 435 ('*j-18)
585.4059	**3β,20R,22R-triHCA** [7]	D/NM	9.32 (4.93)	0.48 (0.38)	ND	0.64 (0.43)	Semi-quantitative[7]	151 (*b_1-12), 163 (*b_3-28), 325 ('*e), 327 (*e'), 353 ('*f-16), 355 (*f'-16), 419 ('*j-36), 437 ('*j-18)
585.4059	**isomer of triHCA** [7]	D/NM	ND	D/NM	ND	ND	Not quantified	163 (*b_3-28), 385, 397, 415, 453, 471

D/NM, detected but not measured. ND, not detected. Authentic standards are available for each metabolite unless otherwise noted. An asterisk preceding a fragment describing letter indicates that the fragment-ion has lost the pyridine ring. A prime before the fragment describing letter indicates that the fragment-ion is deficient in a hydrogen atom compared to a similar fragment formed by a homolytic cleavage, A prime after the fragment describing letter indicates that the fragment-ion has gained a hydrogen atom compared to a similar fragment formed by homolytic cleavage. See Supplemental Figure S1C for examples.

[1]Extraction of oxysterols was performed according to methods designed primarily for brain and liver without further validation.

[2]Single outlier removed.

[3]Ring-oxysterols were not the focus of this study, and their measurement is only semi-quantitative.

[4]20S-HC and 24S-HC give chromatographic peaks that were not completely resolved so were not quantified.

[5]Previous studies have shown $[^2H_7]$24R/S-HC to be a satisfactory internal standard for the quantification of side-chain oxysterols and steroid-acids [Yutuc E, et al., 2021, Anal Chim Acta 1154: 338259].

[6]7α,26-diHC and 7α,26-diHCO were not differentiated.

[7]Presumptive identification, no authentic standard available.

[8]Quantification at the MS^3 level.

10.3389/fendo.2022.1031013

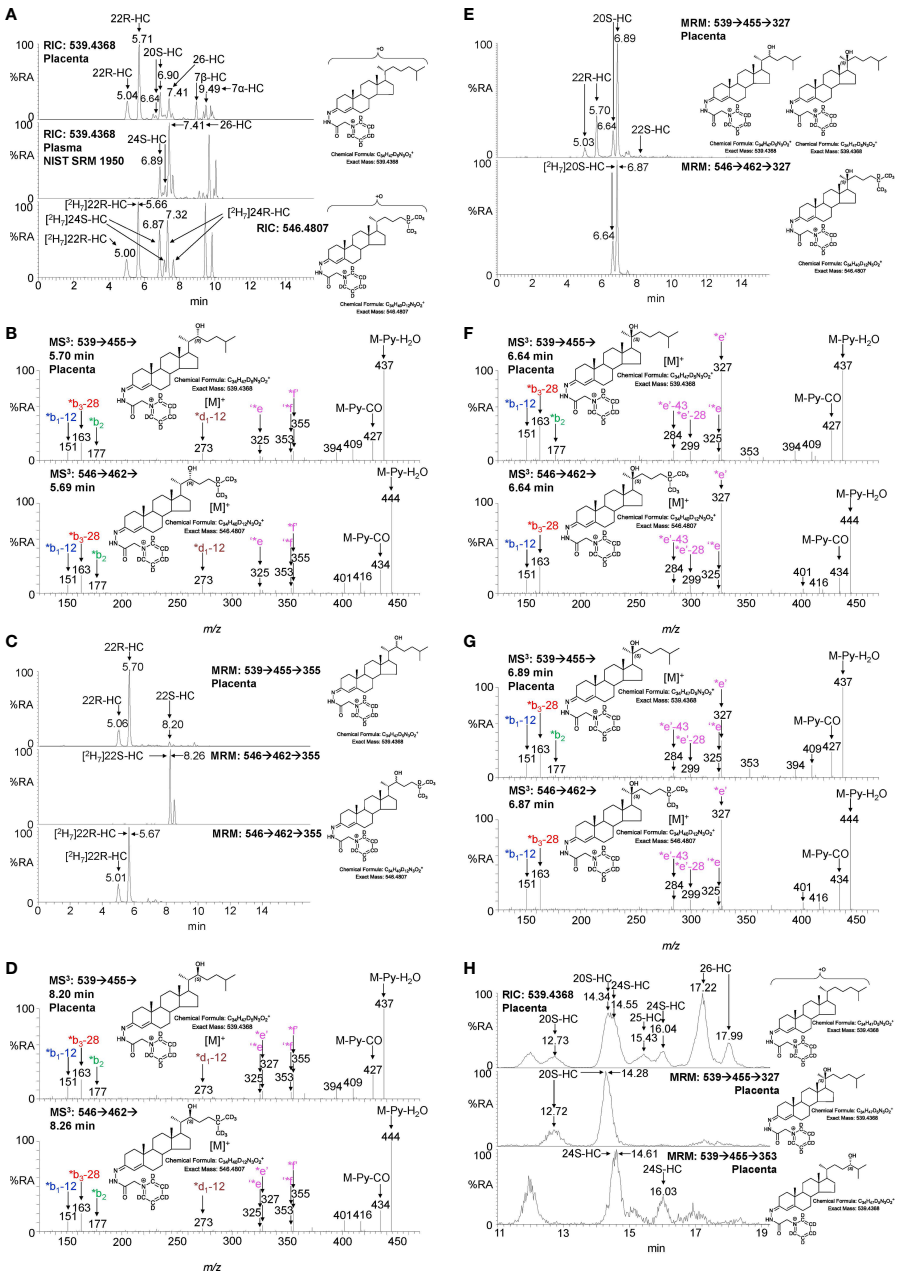

FIGURE 2
LC-MS(MS^n) analysis of GP-derivatised monohydroxycholesterols (HC) in placenta and NIST SRM 1950 plasma. **(A)** Reconstructed ion chromatograms (RICs) for monohydroxycholesterols (HC, *m/z* 539.4368 ± 5 ppm) in placenta (upper panel), NIST SRM 1950 plasma (15) (central panel), and of [$^2H_7$]-labelled standards (546.4807 ± 5 ppm, lower panel). GP-derivatised oxysterols give *syn* and *anti* conformers about the CN double bond which may or may not be resolved. **(B)** MS^3 ([M]$^+$ ➔[M-Py]$^+$ ➔) spectra of 22R-HC identified in placenta (upper panel) and [$^2H_7$] 22R-HC reference standard (lower panel). **(C)** Multiple reaction monitoring-like (MRM) chromatograms targeting 22-HC isomers ([M]$^+$ ➔[M-Py]$^+$ ➔355) found in placental (upper panel), and authentic standards of [$^2H_7$]22S-HC (central panel) and [$^2H_7$]22R-HC (lower panel). **(D)** MS^3 ([M]$^+$ ➔ [M-Py]$^+$ ➔) spectra of 22S-HC identified in placenta (upper panel) and [$^2H_7$]22S-HC reference standard (lower panel). **(E)** MRM-like chromatograms targeting 20S-HC ([M]$^+$ ➔[M-Py]$^+$ ➔327) in placenta (upper panel) and [$^2H_7$]20S-HC authentic standard (lower panel). **(F, G)** MS^3 ([M]$^+$ ➔[M-Py]$^+$ ➔) spectra of *syn* and *anti* conformers of 20S-HC identified in placenta (upper panels) and of [$^2H_7$]20S-HC reference standard (lower panels). **(H)** 20S-HC and 24S-HC can be resolved *via* MRM but not by chromatography alone even when using an extended chromatographic gradient (37 min). Peaks corresponding to 20S-HC and 24S-HC coalesce in the RIC for their [M]$^+$ ions (upper panel), but are resolved by their specific MRMs, i.e. 20S-HC ([M]$^+$ ➔[M-Py] ➔327, central panel) and 24S-HC ([M]$^+$ ➔[M-Py]$^+$ ➔353, lower panel). See Supplemental Figure S3 for MS^3 spectra of 24S-HC. As data was collected during different sessions, 17 min gradient chromatograms **(A, C, E)**, have been aligned to the peak corresponding to 26-HC in NIST SRM 1950 plasma.

for the additional presence an intense pair of peaks corresponding to the *syn* and *anti* conformers of [$^2H_5$]GP-derivatised 22R-HC in the placental sample. Note *syn* and *anti* conformers are a consequence of GP-derivatisation at C-3 of the sterol A-ring (see Supplemental Figure S1B). 22R-HC is usually only a minor oxysterol in adult plasma/serum (14, 16) and is essentially absent in the NIST SRM 1950 plasma sample (representative of the adult population of the USA) illustrated here (15). The observation of 22R-HC in placenta is not surprising as CYP11A1, the enzyme which generates this oxysterol in the pathway from cholesterol to pregnenolone, is abundant in placenta (2, 17). The identity of the two early eluting peaks was confirmed by reference to [$^2H_7$]22R-HC authentic standard which co-elutes and gives an identical MS^3 ($[M]^+ \rightarrow [M\text{-}Py]^+ \rightarrow$, where Py is pyridine) fragmentation pattern (Figures 2A, B). A major advantage of the GP-derivatisation method is that unlike the un-derivatised $[M+H]^+$, $[M+NH_4]^+$ or $[M-(H_2O)_n+H]^+$ ion, the $[M]^+$ ion of the GP-derivative gives a structurally informative MS^3 spectrum. The fragmentation of GP-derivatised oxysterols has been described in detail elsewhere (18, 19). In brief, a 3β-hydroxy-5-ene function in the parent structure, with no additional substitutions on the ring system, gives following cholesterol oxidase treatment, GP derivatisation and MS^3, a pattern of low-*m/z* fragment ions at 151.1 (*b_1-12), 163.1 (*b_3-28) and 177.1 (*b_2) and a mid-*m/z* fragment ion at 325.2 ('*e, Supplemental Figure S1C). A characteristic, but not unique, fragment ion of 22R-HC is at *m/z* 355.3 (*f', Figure 2B and Supplemental Figure S2A), this appears alongside a satellite peak at *m/z* 353.3 ('*f). By generating a multiple reaction monitoring (MRM)-like chromatogram $[M]^+ \rightarrow [M\text{-}Py]^+ \rightarrow$355.3 the 22R-HC peaks in placenta are highlighted (Figure 2C upper panel). A minor unknown pair of peaks were also observed eluting much later in the MRM chromatogram. Their MS^3 spectra suggests that these correspond to the 22S-epimer (Figure 2D). This was confirmed by analysis of [$^2H_7$]22S-HC which gave an identical MS^3 fragmentation pattern and co-eluted with the endogenous molecule.

In many LC-MS/MS studies oxysterols are identified by MRM where the transition is often non-specific (16, 20). This provides high sensitivity but relies on chromatographic separation of isomers and co-elution with isotopic labelled standards (21). In an initial interpretation of the data presented in Figure 2A (upper panel), the peak at 6.90 min was assumed to be 24S-HC, presumably from contaminating blood. However, closer scrutiny of the chromatogram and relevant MS^3 spectra suggested that the earlier eluting peak 6.64 min was one of the *syn* or *anti* conformers of 20S-HC. 20S-HC has a characteristic MS^3 fragmentation spectrum with a major fragment ion at 327.2 (*e', Figure 2F and Supplemental Figure S2B). By generating a MRM chromatogram for $[M]^+ \rightarrow [M\text{-}Py]^+ \rightarrow$327.2, two peaks corresponding to the *syn* and *anti* conformers of 20S-HC are revealed (Figure 2E). The second peak co-elutes with 24S-HC, of which minor quantities are present as revealed by the 24S-HC characteristic fragment ion at *m/z* 353.3 ('*f, Figure 2G upper panel & Supplemental Figure S1D). However, by extending the chromatographic gradient and by exploiting the specific MRM chromatograms i.e. $[M]^+ \rightarrow [M\text{-}Py]^+ \rightarrow$327.2 for 20-HC and $[M]^+ \rightarrow [M\text{-}Py]^+ \rightarrow$353.3 for 24-HC, the two isomers can be partially resolved (Figure 2H, see Supplemental Figure S3 for the MS^3 spectrum of 24S-HC). Fortuitously, as both 20S-HC and 24S-HC give *syn* and *anti* conformers following GP-derivatisation, the first peak of 20S-HC (12.73 min) is completely resolved from both peaks of 24S-HC and it is only the second peak of 20S-HC and the first peak of 24S-HC that partially co-elute, leaving the second peak of 24S-HC (16.04 min) completely resolved from 20S-HC.

As is evident from Figures 2A, H, other monohydroxycholesterols were also observed in placenta including (25R)26-hydroxycholesterol (26-HC, also known by the non-systematic name 27-hydroxycholesterol, 27-HC) and 7α-hydroxycholesterol (7α-HC). MS^3 spectra are shown in Supplemental Figure S3. 7β-Hydroxycholesterol (7β-HC) was also observed, this like 7α-HC may be endogenous, but can also be formed during sample preparation by *ex vivo* oxidation (22). In placenta minor quantities of (25R)26-hydroxycholest-4-en-3-one and 22R-hydroxycholest-4-en-3-one, the natural 3-oxo-4-ene relatives of 26-HC and 22R-HC, respectively, were also observed, but are the subject of a separate report (23).

3.1.2 Dihydroxycholesterols, trihydroxycholesterols, pregnenolone and progesterone

The second step in the conversion of cholesterol to pregnenolone by CYP11A1 is the generation of 20R,22R-diHC from 22R-HC (Figure 1). The RIC (*m/z* 555.4317 ± 5 ppm) for dihydroxycholesterols reveals two major peaks which appear at retention times, and give identical MS^3 ($[M]^+ \rightarrow [M\text{-}Py]^+ \rightarrow$) spectra, to the authentic standard of 20R,22R-diHC and are identified as the *syn* and *anti* conformers of the GP-derivative (Figures 3A, B). The MS^3 fragmentation pattern shows features of both 20-HC (*e', *m/z* 327.2, Supplemental Figure S2C) and 22-HC (*f-16, *m/z* 355.3, Supplemental Figure S2D) and to search for possible epimers of 20R,22R-diHC, MRM-like chromatograms were constructed for the transitions $[M]^+ \rightarrow [M\text{-}Py]^+ \rightarrow$327.2 and $[M]^+ \rightarrow [M\text{-}Py]^+ \rightarrow$355.3 (Figure 3A). A minor peak was observed at 5.04 min, but the MS^3 fragmentation pattern corresponded to a different isomer (x,y-diHC), possibly 22,23-dihydroxycholesterol (22,23-diHC, Figures 3C upper panel, and Supplemental Figure S2E). Unsurprisingly, when a search was made for pregnenolone by constructing the appropriate RIC (*m/z* 450.3115) this steroid was evident as was progesterone (*m/z* 448.2959), its HSD3B1 oxidised metabolite, in the fraction not treated with cholesterol oxidase i.e. fraction B (Figures 3D, E). Besides 20R,22R-diHC and the presumptively identified 22,23-diHC, low levels of 7α,(25R)26-dihydroxycholesterol (7α,26-diHC) were also found in placenta (Figures 3A, C).

20R,22R-diHC extracted from placenta gives intense signals in LC-MS and based on this and on the additional presumptive

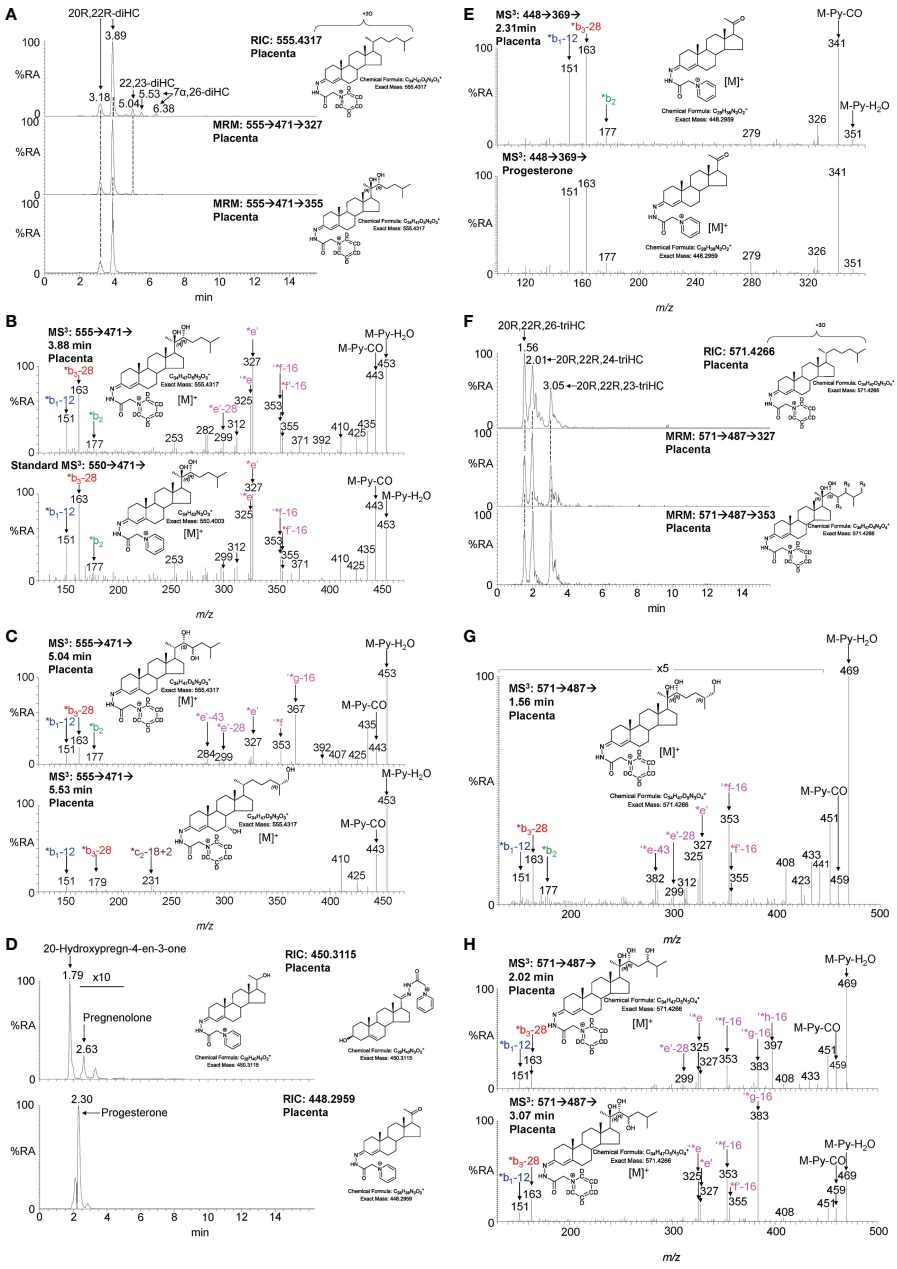

FIGURE 3
LC-MS(MS^n) analysis of GP-derivatised 20R,22R-diHC and its metabolites in placenta. **(A)** RIC (*m/z* 555.4317 ± 5 ppm) corresponding to the $[M]^+$ ion of dihydroxycholesterols (diHC, upper panel). MRM-like chromatograms targeting 20R,22R-diHC ($[M]^+$ ➔$[M\text{-}Py]^+$ ➔327, central panel) and ($[M]^+$ ➔$[M\text{-}Py]^+$ ➔355, lower panel). **(B)** MS^3 ($[M]^+$ ➔$[M\text{-}Py]^+$ ➔) spectra of 20R,22R-diHC from placenta (upper panel) and of an authentic standard (lower panel). **(C)** MS^3 ($[M]^+$ ➔$[M\text{-}Py]^+$ ➔) spectra of other dihydroxycholesterols found in placenta, possibly 22,23-diHC (upper panel) and 7α,26-diHC (lower panel). **(D)** RICs (*m/z* 450.3115) corresponding to pregnenolone (upper panel) and *m/z* 448.2959 corresponding to progesterone. **(E)** MS^3 ($[M]^+$ ➔$[M\text{-}Py]^+$ ➔) spectra of progesterone from placenta (upper panel) and of the reference standard (lower panel). **(F)** RIC (*m/z* 571.4266 ± 5 ppm) corresponding to the $[M]^+$ ion of trihydroxycholesterols (triHC, upper panel). MRM-like chromatograms targeting 20R,22R,x-triHC ($[M]^+$ ➔$[M\text{-}Py]^+$ ➔327, central panel) and ($[M]^+$ ➔$[M\text{-}Py]^+$ ➔353, lower panel). In the structure shown in the lower panel, one of R_1, R_2 or R_3 is a hydroxy group, the other two are hydrogens. **(G)** MS^3 ($[M]^+$ ➔$[M\text{-}Py]^+$ ➔) spectrum of the trihydroxycholesterol found in placenta and commensurate with the 20R,22R,26-triHC structure. **(H)** MS^3 ($[M]^+$ ➔$[M\text{-}Py]^+$ ➔) spectra of other trihydroxycholesterols with possible structures of 20R,22R,24-triHC (upper panel) and 20R,22R,23-triHC. In the absence of authentic standards 20R,22R stereochemistry is assumed on the presumption that the triHCs are derived from 20R,22R-diHC.

identification of 22,23-diHC, it is likely that other hydroxylase activities are present in placenta besides those normally associated with CYP11A1, potentially resulting in the formation of trihydroxycholesterols (triHC). The RIC for triHC (*m/z* 571.4266 ± 5 ppm) reveals three major peaks (Figure 3F upper panel). To tighten the search for hydroxylated metabolites of 20R,22R-diHC, MRM-like chromatograms were generated for the major side-chain cleavage fragment ions associated with the 20R,22R-diHC structure i.e. $[M]^+ \rightarrow [M\text{-}Py]^+ \rightarrow 327.2$, $[M]^+ \rightarrow [M\text{-}Py]^+ \rightarrow 353.3$ (cf. Figure 3B). Again, three major peaks were evident in these chromatograms. Interrogation of the respective MS^3 spectra suggested isomers of 20,22,x-triHC, where x is the location of an additional hydroxy group on the side-chain. Considering the spectrum of the last eluting isomer at 3.05 min (Figures 3F, H lower panel), besides pairs of fragment ions at *m/z* 325/327 ('*e/*e'), *m/z* 353/355 ('*f-16/*f-16) a dominating fragment ion is observed at *m/z* 383 ('*g-16), this pattern is consistent with a 20R,22R,23-triHC isomer (Supplemental Figure S2F cf. S2C). Considering the isomer eluting second at 2.01 min (Figure 3F), the MS^3 spectrum shows an additional fragment ion at *m/z* 397 ('*h-16, Figure 3H upper panel); the structure that explains this fragment ion formation most easily is 20R,22R,24-triHC (Supplemental Figure S2G, cf. S2C & S2D). The MS^3 spectrum of the first eluting peak at 1.56 min (Figure 3G) does not show the fragment-ions at *m/z* 383 or 397 (Figure 3H), suggesting that the extra hydroxy group does not encourage additional side-chain fragmentation. The most likely structures for this isomer are 20R,22R,26-triHC or perhaps 20R,22R,25-triHC (Supplemental Figure S2H, I, cf. S2C & S2D). Note, authentic standards are not available for the 20,22,x-triHC isomers and stereochemical assignments are made based on biosynthetic considerations. As was the situation with 22R-HCO, a minor proportion of 20R,22R-dihydroxysterols are found as the 3-oxo-4-ene, i.e. 20R,22R-dihydroxycholest-4-en-3-one (20R,22R-diHCO) (23).

3.1.3 Cholestenoic acids

Sterol 27-hydroxylase (CYP27A1) is the enzyme that introduces both (25R)26-hydroxy and (25R)26-carboxy groups to sterols (Figure 1) (24), it is expressed in trophoblast cells of the placenta (25). We identify 26-HC (Figures 2A, H; Supplemental Figure S3D) and 3β-hydroxycholest-5-en-(25R)26-oic acid (3β-HCA, Supplemental Figure S4) in placenta, and there is the possibility that 20R,22R-diHC may be a substrate for CYP27A1 and be metabolised *via* 20R,22R,26-triHC to the C_{27} bile acid 3β,20R,22R-trihydroxycholest-5-en-(25R)26-oic acid (3β,20R,22R-triHCA) in placenta (Figure 1). The RIC appropriate for 3β,20R,22R-triHCA (*m/z* 585.4059 ± 5ppm) reveals two major and a minor peak (Figure 4A) of which only the first gives an MS^3 spectrum compatible with a 3β,20R,22R-triHCA structure (Figure 4B & Supplemental Figure S2J & K, cf. Supplemental Figure S2H, I). The similarity between the MS^3 spectra of 20R,22R-diHC, and the presumptively identified 20R,22R,26-triHC and 3β,20R,22R-triHCA can be visualised in Figure 4C where the low-middle *m/z* range of the three spectra are shown on the same *m/z* scale. While the low-middle *m/z* range provides evidence for the 20,22-dihydroxy structural motif (presumably 20R,22R-) the high *m/z* range (Figure 4B) is indicative of a C-26 acid. Sterol acids show characteristic neutral losses from the $[M\text{-}Py]^+$ ion corresponding to the net loss of $H_2CO_2 + n(H_2O)$, where n is the number of OH groups on the sterol beyond that derivatised at C-3 (19). In Figure 4B we see such losses giving fragments at *m/z* 437 ($M\text{-}Py\text{-}H_2O\text{-}H_2CO_2$ i.e. '*j-18) and *m/z* 419 ($M\text{-}Py\text{-}2H_2O\text{-}H_2CO_2$ i.e. '*j-36). These fragment ions are associated with satellite peaks at *m/z* 440 ($[M\text{-}Py\text{-}61]^+$ and 422 ($[M\text{-}Py\text{-}79]^+$) providing a pattern characteristic of a trihydroxycholestenoic acid (See Supplemental Figure S2L). Note, the third hydroxy group is the site of derivatisation. The other two chromatographic peaks give almost identical MS^3 spectra (Figure 4D) presumably *syn* and *anti* conformers of a second isomer whose structure is not obvious from the MS^3 spectra, although fragment-ions at *m/z* 385, 397 and 471 are probably structurally significant.

Cholestenoic acids are intermediates in bile acid biosynthesis pathways (26–28). In the route towards C_{24} acids, C_{27} acids become converted to their CoA-thioesters by bile acid CoA-synthetase (BACS, SLC27A5), stereochemistry at C-25 is inverted by α-methylacyl-CoA racemase (AMACR) and a double bond introduced at Δ^{24} with *trans* geometry by acyl-CoA oxidase 2 (ACOX2, see Figure 1) (27). The next steps are catalysed by D-bifunctional protein (DBP, HSD17B4) and lead to a C-24 oxo group. Beta-oxidation by sterol carrier protein 2 (SCP2) then gives a C_{24} CoA-thioester which is finally amidated with glycine or taurine or hydrated to give the C_{24} acid (27). In bioanalysis, intermediates are almost always observed as the carboxylic acids rather than the thioesters (28). Following this pathway, the CoA-thioester of 3β,20R,22R-triHCA would be isomerised from the 25R-epimer to one with 25S-stereochemistry which would then be oxidised to the CoA-thioester of 3β,20R,22R-trihydoxycholest-5,24-dienoic acid (3β,20R,22R-triH-Δ^{24}-CA, Figure 1). Shown in Figure 4E is the RIC (*m/z* 583.3902 ± 5 ppm) appropriate to the $[M]^+$ ion of 3β,20R,22R-triH-Δ^{24}-CA, along with MRM-like chromatograms characteristic of sterols with 20- and 22-hydroxylation of the side-chain. One major chromatographic peak is evident at 2.20 min, and the MS^3 ($[M]^+ \rightarrow [M\text{-}Py]^+ \rightarrow$) spectrum associated with this peak (Figure 4F) resembles, in the low to middle *m/z* range, that of 3β,20R,22R-triHCA (Figure 4B), however, the fragment-ion observed at *m/z* 355 (*f-16) in spectrum of 3β,20R,22R-triHCA is replaced by one at *m/z* 371 (*f) in the spectrum shown Figure 4F. This spectrum is compatible with the 3β,20R,22R-triH-Δ^{24}-CA structure (see Supplemental Figures S2M–O). Further evidence for the MS^3 spectrum presented in Figure 4F corresponding to 3β,20R,22R-triH-Δ^{24}-CA is the presence of fragment ions characteristic of sterol acids, '*j-18 ($M\text{-}Py\text{-}H_2O\text{-}H_2CO_2$) at *m/z* 435 and '*j-36 ($M\text{-}Py\text{-}2H_2O\text{-}H_2CO_2$) at *m/z* 417. These fragment ions are associated with satellite peaks at *m/z* 438 ($[M\text{-}Py\text{-}61]^+$ and 420

10.3389/fendo.2022.1031013

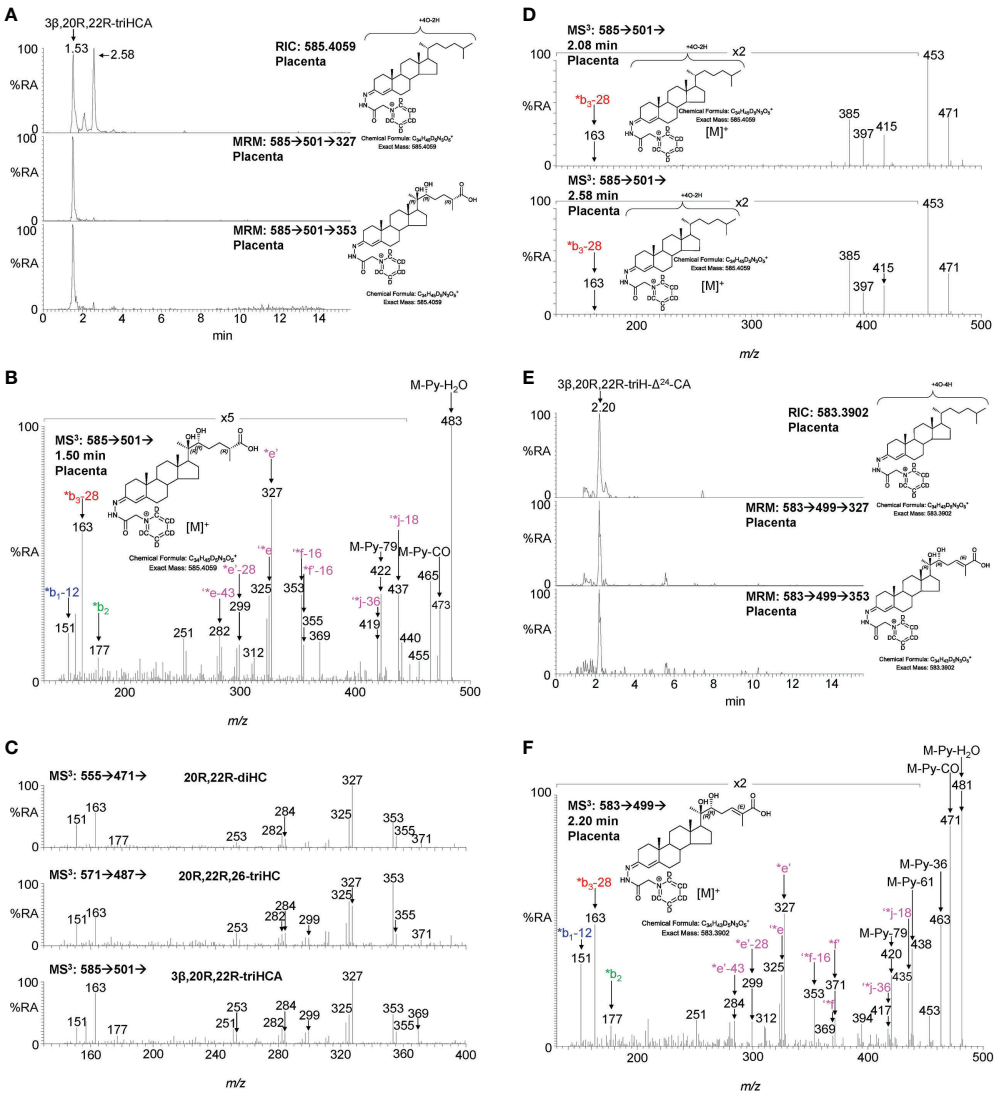

FIGURE 4
LC-MS(MS^n) analysis of GP-derivatised 3β,20R,22R-triHCA, its isomers and of 3β,20R,22R-triH-Δ^{24}-CA in placenta. **(A)** RIC (*m/z* 585.4059 ± 5 ppm) corresponding to the $[M]^+$ ion of trihydroxycholestenoic acids (upper panel). MRM-like chromatograms targeting 3β,20R,22R-triHCA ($[M]^+$ ➔$[M\text{-}Py]^+$ ➔327, central panel) and ($[M]^+$ ➔$[M\text{-}Py]^+$ ➔353, lower panel). **(B)** MS^3 ($[M]^+$ ➔$[M\text{-}Py]^+$ ➔) spectrum postulated to correspond to 3β,20R,22R-triHCA. **(C)** Comparison of MS^3 ($[M]^+$ ➔$[M\text{-}Py]^+$ ➔) spectra of 20R,22R-diHC (upper panel) with spectra postulated to correspond to 20R,22R,26-triHC (central panel) and 3β,20R,22R-triHCA (lower panel) over the *m/z* range 130 – 400. **(D)** MS^3 spectra of two other isomers but the spectra do not appear to be of cholestenoic acids. **(E)** RIC (*m/z* 583.3902 ± 5 ppm) corresponding to the $[M]^+$ ion of a trihydroxycholestadienoic acid (upper panel). MRM-like chromatograms targeting 3β,20R,22R-triH-Δ^{24}-CA ($[M]^+$ ➔$[M\text{-}Py]^+$ ➔327, central panel) and ($[M]^+$ ➔$[M\text{-}Py]^+$ ➔353, lower panel). **(F)** MS^3 ($[M]^+$ ➔$[M\text{-}Py]^+$ ➔) spectrum postulated to correspond to 3β,20R,22R-triH-Δ^{24}-CA. As was the case with 20R,22R,26-triHC in Figure 3, the 20R,22R-stereochemistry is assumed in 3β,20R,22R-triHCA and 3β,20R,22R-triH-Δ^{24}-CA.

($[M\text{-}Py\text{-}79]^+$, see Supplemental Figure S2N). However, as is the case with other postulated structures definitive identification awaits synthesis of the authentic standard. Again, as was the case with 20R,22R,26-triHC, the 20R,22R-stereochemistry is assumed in 3β,20R,22R-triHCA and 3β,20R,22R-triH-Δ^{24}-CA. Note the ultimate C_{24} bile acid 3β,20R,22R-trihydroxychol-5-enoic acid was not observed, perhaps due to low expression of HSD17B4 or SCP2 in placenta.

3.2 Identification of oxysterols in cord and maternal plasma

To investigate if the placental oxysterols are transported to the fetus, umbilical cord plasma derived from umbilical cord blood was analysed for oxysterols. The data was compared to the oxysterol profiles in plasma from maternal blood, taken 1 - 2 day before elective caesarean section and plasma from “control”

non-pregnant females. As might be expected, the oxysterol profile of cord plasma resembles that of non-pregnant females, but with the additional presence of CYP11A1-derived oxysterols. 22R-HC is present in both cord and maternal plasma but is absent from controls (Figures 5A, B, 6A–C; Table 1). If present, 20S-HC is at levels in cord, maternal and control plasma samples below the limit of detection (0.1 ng/mL). The dihydroxycholesterol 20R,22R-diHC is the dominant oxysterol in cord plasma, it is also a major oxysterol in maternal plasma but is absent from control plasma (Figures 5C, D, 6D–F). Presumptively identified 20R,22R,26-triHC was near the limit of quantification in both cord and maternal plasma but was absent from controls (Figures 5E, F, 6G, H). The presumptively identified C_{27} bile acid 3β,20R,22R-triHCA was evident in cord plasma and just detected in maternal plasma but was absent from control plasma (Figures 5G, H, 7A–C). Presumptively identified 3β,20R,22R-triH-Δ^{24}-CA was only detected in cord plasma (Supplemental Figures S5A, B).

Besides the oxysterols discussed above, the profile of cord and maternal plasma was investigated for other oxysterols and sterol acids routinely found in adult plasma, this data is included in Table 1. While it was possible to make quantitative measurements for mono- and di-hydroxycholesterols thanks to the availability of authentic standards, the absence of standards for 20R,22R,26-triHC and 3β,20R,22R-triHCA means that the values determined for these metabolites are semi-quantitative, but by using the same internal standard for quantification across samples should give reliable measurements for relative quantification across the sample groups.

In cord plasma, but not plasma from pregnant and non-pregnant females, 22R-HCO was found but at a much lower level than 22R-HC. 20R,22R-diHCO was found in both cord plasma and plasma from pregnant females, but not non-pregnant females. Further details are reported elsewhere (23).

3.3 Identification of oxysterols in amniotic fluid

Amniotic fluid is derived from maternal plasma but also contains progressively more fetal urine as pregnancy continues. One of its functions is to facilitate the exchange of biochemicals between mother and fetus. Based on the data from analysis of placenta and cord plasma, it is reasonable to expect to find 22R-HC and its down-stream metabolites in amniotic fluid. As in cord and maternal blood 22R-HC (Figures 6A–C), 20R,22R-diHC (Figures 6D–F), 20R,22R,26-triHC (Figures 6G, H) and 3β,20R,22R-triHCA (Figures 7A–C) were identified and quantified in amniotic fluid (Table 1). Presumptively identified 3β,20R,22R-triH-Δ^{24}-CA was also detected but not quantified (Supplemental Figures S5C, D).

3.4 Relative quantification between samples groups

As mentioned above although the measurement of some of the metabolites of 22R-HC is only semi-quantitative, relative values are likely to be accurate (Table 1). Shown in Figure 8 are plots displaying the quantities determined in the different samples for 22R-HC and its dominant metabolites. With respect to these metabolites, cord plasma is very different to control plasma from non-pregnant females with statistical differences also observed between cord and maternal plasma for 20R,22R-diHC and 3β,20R,22R-triHCA.

3.5 Quantification of other oxysterols

Besides the oxysterols discussed in the previous section, other oxysterols typically measured by the charge-tagging approach were also measured and are presented in Table 1 (11, 14, 19). Note the values for the oxysterols and sterol acids for which there is no authentic standard were quantified against [$^2H_7$]24R/S-HC and are only semi-quantitative values.

4 Discussion

In the current study we have investigated the oxysterol profile of placenta, cord plasma, maternal plasma, non-pregnant female plasma (control plasma) and amniotic fluid. In each of the pregnancy samples we identify metabolites derived from CYP11A1 which are essentially absent from non-pregnant females (Figure 8; Table 1). There are two significant findings from the current study. Firstly, the rediscovery of 20S-HC and the discovery of 22S-HC in human placenta (7), and secondly the uncovering of a shunt pathway for 22R-HC metabolism to C_{27} bile acids.

20S-HC is a controversial oxysterol as it has been detected in very few analytical studies (7, 8, 29, 30) despite being biologically active *in vitro*. 20S-HC, like 22R-HC, is a ligand to the liver X receptors α and β (LXRα, LXRβ) (31) and to the retinoic acid receptor-related orphan receptor γ (RORγ) (32), but unlike 22R-HC, activates the G protein-coupled receptor (GPCR) Smoothened (SMO), a key protein in the hedgehog signalling pathway, required for proper cell differentiation in the embryo (33, 34). 20S-HC also inhibits the processing of SREBP-2 (sterol regulatory element-binding protein 2) to its active form as the master transcription factor regulating cholesterol biosynthesis (35, 36), presumably by binding to INSIG (insulin induced gene) in a manner similar to other side-chain hydroxycholesterols (37). Recently, 20S-HC has been identified as a ligand to the sigma 2 (σ2) receptor (38), also known as transmembrane

10.3389/fendo.2022.1031013

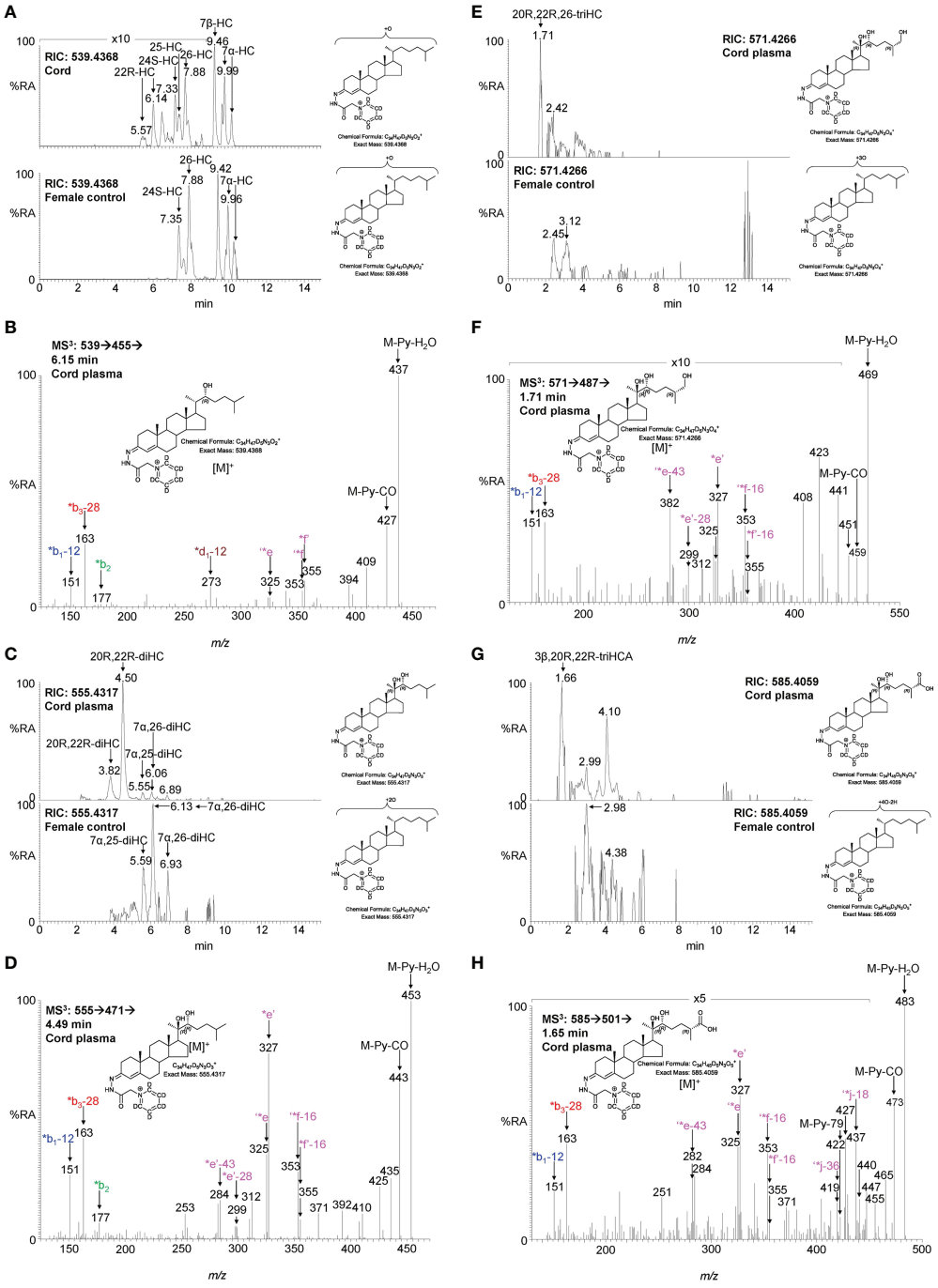

FIGURE 5
LC-MS(MS^n) analysis of GP-derivatised oxysterols in umbilical cord plasma. **(A)** RICs for monohydroxycholesterols (*m/z* 539.4368 ± 5 ppm) in cord (upper panel) and control non-pregnant female plasma (lower panel). **(B)** MS^3 ([M]$^+$ ➔[M-Py]$^+$ ➔) spectrum of 22R-HC from cord plasma. **(C)** RICs for dihydroxycholesterols (*m/z* 555.4317 ± 5 ppm) in cord (upper panel) and control female plasma (lower panel). **(D)** MS^3 ([M]$^+$ ➔[M-Py]$^+$ ➔) spectrum of 20R,22R-diHC from cord plasma. **(E)** RICs for trihydroxycholesterols (*m/z* 571.4266 ± 5 ppm) in cord (upper panel) and control female plasma (lower panel). **(F)** MS^3 ([M]$^+$ ➔[M-Py]$^+$ ➔) spectrum postulated to correspond to 20R,22R,26-triHC. **(G)** RIC (*m/z* 585.4059 ± 5 ppm) corresponding to the [M]$^+$ ion of trihydroxycholestenoic acids in cord plasma (upper panel) and control female plasma. **(H)** MS^3 ([M]$^+$ ➔[M-Py]$^+$ ➔) spectrum postulated to correspond to 3β,20R,22R-triHCA. Note, cord and control female plasma were analysed using a different LC column (same type, different batch) to placenta.

10.3389/fendo.2022.1031013

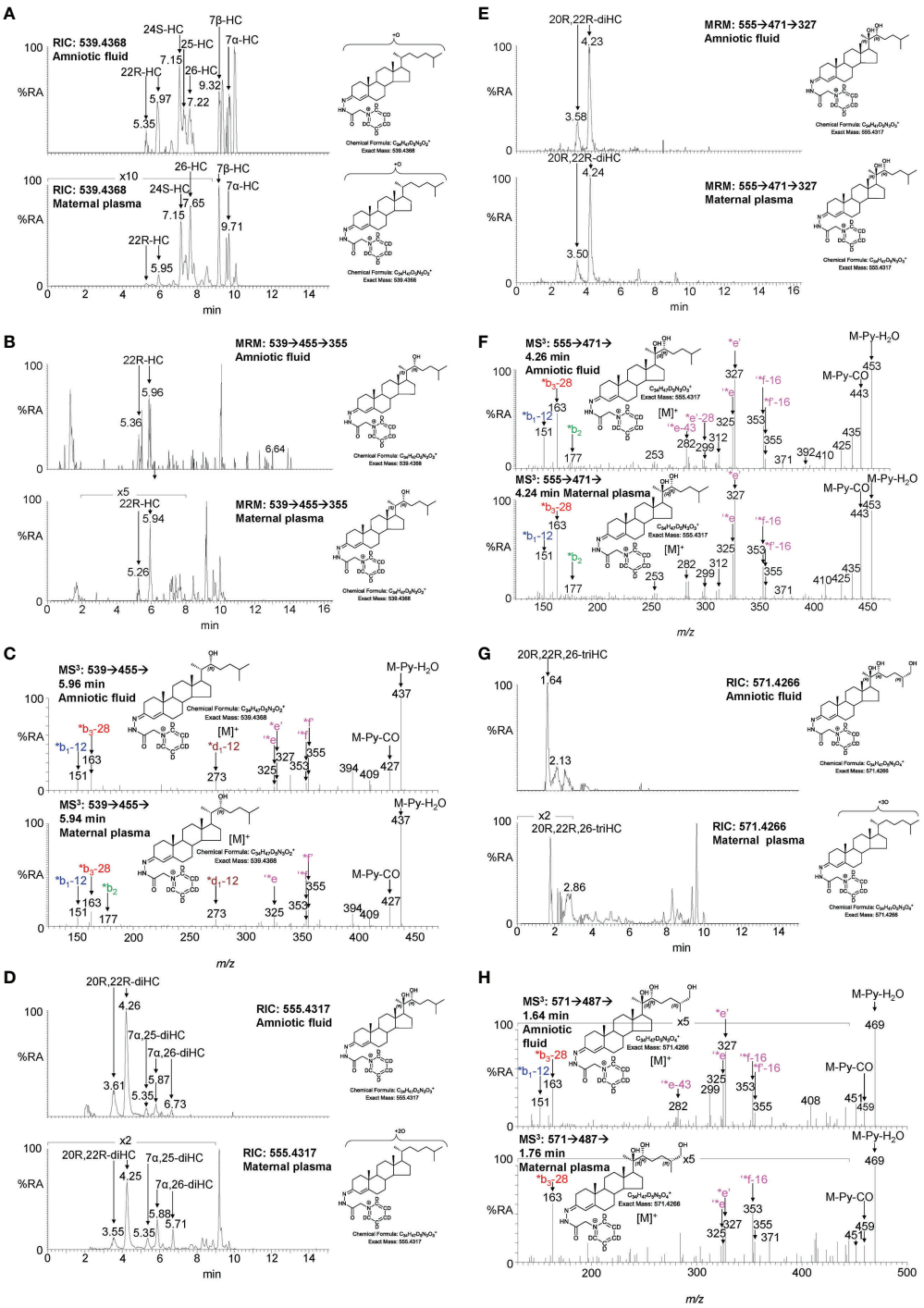

FIGURE 6
LC-MS(MS^n) analysis of GP-derivatised oxysterols in amniotic fluid and plasma from pregnant females (maternal plasma). **(A)** RICs for monohydroxycholesterols (*m/z* 539.4368 ± 5 ppm) in amniotic fluid (upper panel), and in plasma from pregnant females (lower panel). **(B)** MRM-like ($[M]^+$ ➔$[M\text{-}Py]^+$ ➔355) chromatograms targeting 22-HC in amniotic fluid (upper panel) and in plasma from pregnant females (lower panel). **(C)** MS^3 ($[M]^+$ ➔$[M\text{-}Py]^+$ ➔) spectra of 22R-HC identified in amniotic fluid (upper panel) and in plasma from pregnant females (lower panel). **(D)** RIC (*m/z* 555.4317 ± 5 ppm) corresponding to the $[M]^+$ ion of dihydroxycholesterols identified in amniotic fluid (upper panel) and in plasma from pregnant females (lower panel). **(E)** MRM-like chromatograms targeting 20R,22R-diHC ($[M]^+$ ➔$[M\text{-}Py]^+$ ➔327) in amniotic fluid (upper panel) and in plasma from pregnant females (lower panel). **(F)** MS^3 ($[M]^+$ ➔$[M\text{-}Py]^+$ ➔) spectra of 20R,22R-diHC in amniotic fluid (upper panel) and in plasma from pregnant females (lower panel). **(G)** RICs for trihydroxycholesterols (*m/z* 571.4266 ± 5 ppm) in amniotic fluid (upper panel) and in plasma from pregnant females (lower panel). **(H)** MS^3 ($[M]^+$ ➔$[M\text{-}Py]^+$ ➔) spectra of the trihydroxycholesterols found in amniotic fluid (upper panel) and in plasma from pregnant females (lower panel) commensurate with the 20R,22R,26-triHC structure.

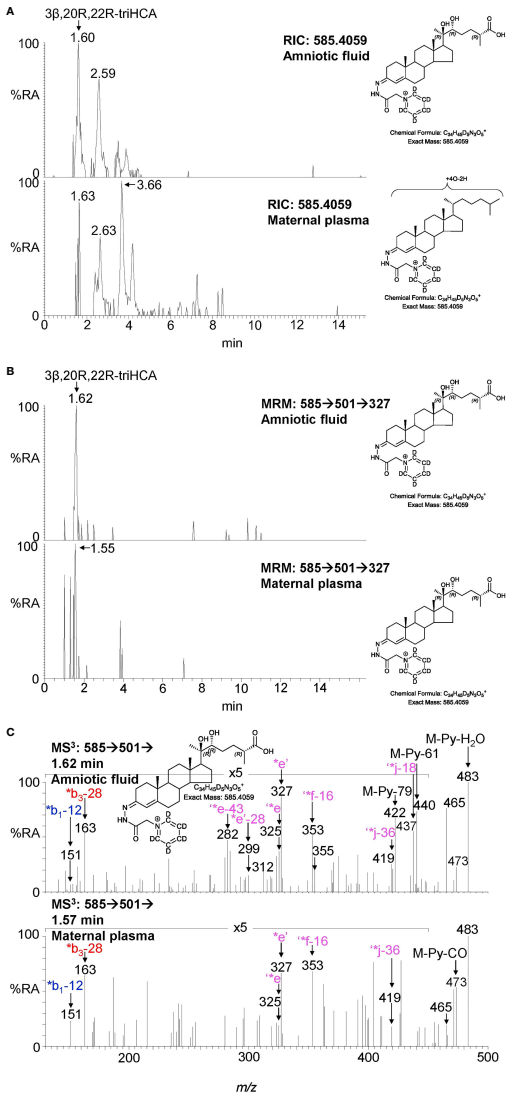

FIGURE 7
LC-MS(MS^n) analysis of GP-derivatised trihydroxycholestenoic acids found in amniotic fluid and plasma from pregnant females (maternal plasma). **(A)** RICs (*m/z* 585.4059 ± 5 ppm) corresponding to the $[M]^+$ ion of trihydroxycholestenoic acids found in amniotic fluid (upper panel) and in plasma from pregnant females (lower panel). **(B)** MRM-like ($[M]^+$ ➔$[M\text{-}Py]^+$ ➔327) chromatograms targeting 3β,20R,22R-triHCA in amniotic fluid (upper panel) and in plasma from pregnant females (lower panel). **(C)** MS^3 ($[M]^+$ ➔$[M\text{-}Py]^+$ ➔) spectra postulated to correspond to 3β,20R,22R-tiHCA in amniotic fluid (upper panel) and in plasma from pregnant females (lower panel).

protein 97 (Tmem97), which is expressed in the central nervous system (39), and has been suggested to be a chaperone protein for NPC1 (Niemann Pick C1), the lysosomal cholesterol transport protein (38). The enzyme required to biosynthesise 20S-HC has not been identified, although CYP11A1 has been reported to generate both 20-hydroxyvitamin D_3 and 20,22-dihydroxyvitamin D_3 or 20,23-dihydroxyvitamin D_3 from vitamin D_3 (40, 41). The high level of CYP11A1 in placenta (17), makes this a good candidate enzyme for biosynthesis of 20S-HC. Like 20S-HC, there are few reports of the detection of 22S-HC in biological systems (30), however, 22S-HC has been identified as the sulphate ester in human meconium (10), the earliest stool of a mammalian infant, and in the human cell lines HCT-15 and HCT-116 (42). Unlike 20S-HC and most other side-chain oxysterols, 22S-HC is not an LXR agonist (43), behaving more like an antagonist (44), neither does it activate the Hh signalling pathway through SMO (33).

22R-HC and 20R,22R-diHC are abundant oxysterols in cord plasma and placenta. 20R,22R-diHC, like 22R-HC and 20S-HC, is an LXR ligand and all three appears to have similar activating capacity (45). Although the primary function of the LXRs is considered to be the regulation of cellular cholesterol (46), LXRs

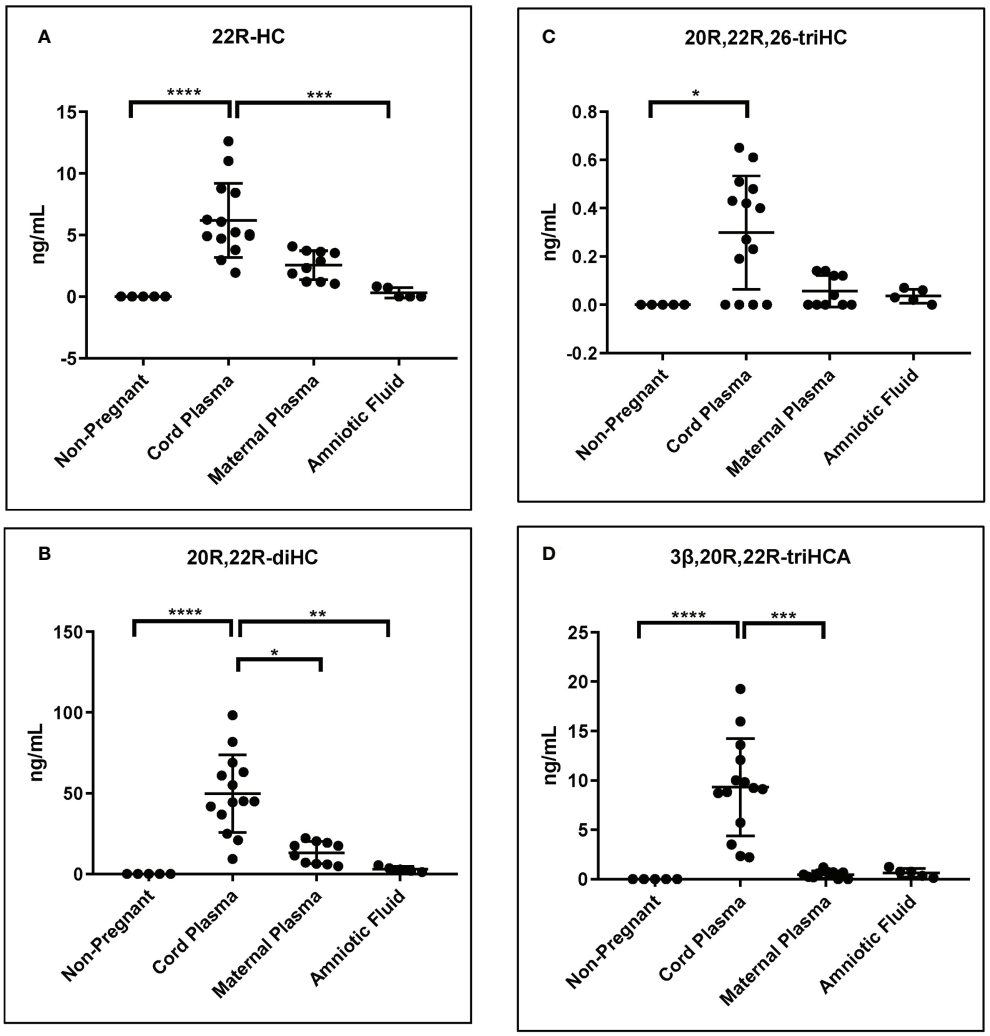

FIGURE 8
Concentration of 22R-HC and downstream metabolites. For each sample type: Control non-pregnant female plasma (plasma, n = 5); cord plasma (n = 14); maternal (pregnant female) plasma (n = 10); and amniotic fluid (n = 5). Concentrations of **(A)** 22R-HC, **(B)** 20R,22R-diHC, **(C)** 20R,22R,26-triHC and **(D)** 3β,20R,22R-triHCA were determined by LC-MS exploiting charge-tagging utilising GP derivatisation. Vales in **(A)** and **(B)** are quantitative (authentic standards available), those in **(C)** and **(D)** are semi-quantitative (authentic standards not available). The band represents the median where the whiskers extend to the most extreme upper and lower data points which are no more than 1.5 times the range between the first and third quartile. Non-parametric Kruskal-Wallis multiple comparisons test was used for comparison of data. *P < 0.05; **P < 0.01, ***P < 0.001 ****P < 0.0001.

also appear to have developmental functions, being required for the development of dopaminergic neurons in midbrain (47). In fact, LXRβ also appears to have a protective role towards dopaminergic neurons, as the synthetic agonist GW3965 protects against the loss of dopaminergic neurons in a Parkinson's disease mouse model (48).

CYP11A1 is an inner mitochondrial membrane protein and catalyses the side-chain cleavage of cholesterol to pregnenolone. The intermediates in this reaction scheme i.e. 22R-HC and 20R,22R-diHC, bind more tightly to CYP11A1 and are converted to pregnenolone at a greater rate than cholesterol (49). It is generally considered that 22R-HC and 20R,22R-diHC remain in the active site until all three oxidation steps are complete (3), however, the abundance of 22R-HC, and the observation of 20R,22R-diHC, in cord plasma, maternal plasma and placenta in this study would argue that this is not always the case.

Pregnenolone is converted to progesterone by HSD3B1 which is localised in both mitochondria and the endoplasmic reticulum (50, 51), and is highly expressed in placenta (52). Progesterone has many roles associated with the establishment and maintenance of pregnancy, including ovulation, uterine and mammary gland development and the onset of labour (53). Progesterone

suppresses spontaneous uterine contractility during pregnancy and, in most mammals, a fall in systemic progesterone is required for the initiation of labour at term. However, in humans, labour occurs in the presence of elevated circulating levels of progesterone. Despite this, disruption of progesterone signalling by the progesterone receptor (PR) antagonist RU486 at any stage of pregnancy results in myometrial contractions and labour, strongly suggesting that reduced progesterone signalling is responsible for labour in women (54). In the current study we have uncovered a shunt pathway that operates in parallel to pregnenolone/progesterone biosynthesis in the placenta (Figure 1). Beyond 20R,22R-diHC we identified three trihydroxycholesterol isomers, one of which gives an MS^3 fragmentation pattern consistent with 20R,22R,26-triHC, and two dihydroxycholestenoic acid isomers one of which gives a fragmentation pattern we assign to 3β,20R,22R-triHCA. A downstream metabolite 3β,20R,22R-triH-Δ^{24}-CA was also presumptively identified. Here we assign stereochemistry based on the assumption of 20R,22R-diHC being the precursor, but we await the chemical synthesis of these metabolites to definitively confirm their identification, this will be required whether LC-MS/MS or gas chromatography - MS is the identification method. However, their presence during pregnancy would define a new pathway of C_{27} bile acid biosynthesis (Figure 1). Most of the metabolites of this pathway are also observed in cord plasma, maternal plasma and amniotic fluid (Table 1). Notably, the amniotic fluid samples were from 16 – 18 weeks of gestation and the other pregnancy samples 37 + weeks indicating a pathway operational throughout pregnancy. CYP27A1 is the likely sterol hydroxylase which will convert 20R,22R-diHC to 20R,22R,26-triHC and on to 3β,20R,22R-triHCA. Like CYP11A1, CYP27A1 is an inner mitochondrial membrane enzyme and is expressed in placenta (6, 25). Although the C_{27} bile acid 3β,20R,22R-triHCA has not previously been identified, a C_{27} bile acid with 22R-hydroxylation has been identified in a patient with Zellweger's syndrome (55). It should be noted that 20S-HC will also act as a substrate for pregnenolone formation *via* a CYP11A1 catalysed reaction (30), presumably *via* 20R,22R-diHC (56). Thus, a potential route for 20S-HC metabolism is through 20R,22R-diHC and on to C_{27} bile acids.

How important is the 20R,22R-diHC shunt pathway? At present we can only speculate, but the LXR-activating capacity of 22R-HC and 20R,22R-diHC and the expression of both LXRα and β during mammalian development makes it tempting to speculate that 20R-HC, 20R,22R-diHC and also 20S-HC by activating LXR, and in the case of 20S-HC by binding to Smo and Tmem97, are important for development of the embryo (Figure 9). Interestingly Tmem97 is a SREBP target gene (57), meaning that 20S-HC is both a Tmem97 ligand and a regulator of its synthesis. Tmem97 is associated with NPC1 in the endosomal-lysosomal compartment linking it to cholesterol transport. Little is known about the biological activities of trihydroxycholesterols and trihydroxycholestenoic acids and it is unknown whether 20R,22R,26-triHC, 3β,20R,22R-triHCA

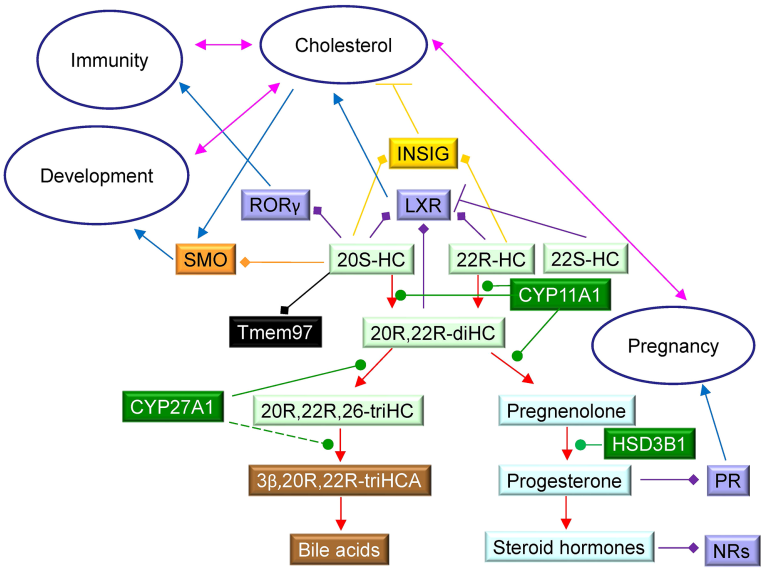

FIGURE 9
Schematic showing some cholesterol metabolites identified in placenta and their interactions with protein receptors. 22R-HC, 22S-HC and 20S-HC are formed from cholesterol, 22R-HC by CYP11A1 which may also be the enzyme that catalyses the formation of 20S-HC. Oxysterols are shown on a light green background, steroids on a light blue background, bile acids on a brown background and enzymes on a dark green background. Nuclear receptors are shown on a purple background, GPCR on an orange background, sigma-2 receptor on a black background and INSIG on a mustard background. Blue arrows indicate a "process", red arrows a chemical reaction, T signifies inhibition of a process, arrows with a diamond arrowhead indicate activation of a receptor, and green oval arrowheads indicate catalysis. Pink double headed arrows link processes.

and 3β,20R,22R-triH-Δ^{24}-CA are simply inactive intermediates on the road to bile acids or biologically active molecules themselves. A final point of note, during the course of this study we found evidence that HSD3B1 can oxidise sterols as well as steroids. Further details are reported elsewhere (23).

Data availability statement

The original contributions presented in the study are included in the article/Supplementary Material. Further inquiries can be directed to the corresponding author. Datasets generated during this study are available in the Open Science Framework repository.

Ethics statement

The studies involving human participants were reviewed and approved by Local ethics committee at Swansea University Medical School. The patients/participants provided their written informed consent to participate in this study.

Author contributions

AD wrote the first draft of the manuscript, acquired, analysed and interpreted the data. EY analysed data and contributed to writing the manuscript by revising it critically for important intellectual content. CT provided essential materials and contributed to writing the manuscript by revising it critically for important intellectual content. YW conceived and designed the work, interpreted the data and contributed to writing the manuscript by revising it critically for important intellectual content. WG conceived and designed the work, interpreted the data and wrote the manuscript. All authors contributed to writing of the manuscript and approved the final version.

Funding

This work was supported by the Biotechnology and Biological Sciences Research Council (BBSRC, grant numbers BB/I001735/1, BB/N015932/1 and BB/S019588/1 to WG, BB/L001942/1 to YW), the European Union through European Structural Funds (ESF), as part of the Welsh Government funded Academic Expertise for Business project (to WG and YW). AD was supported *via* a KESS2 award in association with Markes International from the Welsh Government and the European Social Fund.

Acknowledgments

Dr Peter Grosshans and Steve Smith of Markes International are thanked for helpful discussions. Members of the European Network for Oxysterol Research (ENOR, https://www.oxysterols.net/) are thanked for informative discussions.

Conflict of interest

WG and YW are listed as inventors on the patent "Kit and method for quantitative detection of steroids" US9851368B2. WG, EY, and YW are shareholders in CholesteniX Ltd.

The remaining authors declare that the research was conducted in the absence of any commercial or financial relationships that could be construed as a potential conflict of interest.

Publisher's note

Supplementary material

The Supplementary Material for this article can be found online at: https://www.frontiersin.org/articles/10.3389/fendo.2022.1031013/full#supplementary-material

References

1. Woollett LA. Where does fetal and embryonic cholesterol originate and what does it do? *Annu Rev Nutr* (2008) 28:97–114. doi: 10.1146/annurev.nutr.26.061505.111311

2. Chatuphonprasert W, Jarukamjorn K, Ellinger I. Physiology and pathophysiology of steroid biosynthesis, transport and metabolism in the human placenta. *Front Pharmacol* (2018) 91027. doi: 10.3389/fphar.2018.01027

3. Mast N, Annalora AJ, Lodowski DT, Palczewski K, Stout CD, Pikuleva IA. Structural basis for three-step sequential catalysis by the cholesterol side chain cleavage enzyme CYP11A1. *J Biol Chem* (2011) 286:5607–13. doi: 10.1074/jbc.M110.188433

4. Tuckey RC, Cameron KJ. Catalytic properties of cytochrome p-450scc purified from the human placenta: comparison to bovine cytochrome p-450scc. *Biochim Biophys Acta* (1993) 1163:185–94. doi: 10.1016/0167-4838(93)90180-Y

5. Sun Y, Kopp S, Strutz J, Gali CC, Zandl-Lang M, Fanaee-Danesh E, et al. Gestational diabetes mellitus modulates cholesterol homeostasis in human fetoplacental endothelium. *Biochim Biophys Acta Mol Cell Biol Lipids* (2018) 1863:968–79. doi: 10.1016/j.bbalip.2018.05.005

6. Mistry HD, Kurlak LO, Mansour YT, Zurkinden L, Mohaupt MG, Escher G. Increased maternal and fetal cholesterol efflux capacity and placental CYP27A1 expression in preeclampsia. *J Lipid Res* (2017) 58:1186–95. doi: 10.1194/jlr.M071985

7. Lin YY, Welch M, Lieberman S. The detection of 20S-hydroxycholesterol in extracts of rat brains and human placenta by a gas chromatograph/mass spectrometry technique. *J Steroid Biochem Mol Biol* (2003) 85:57–61. doi: 10.1016/S0960-0760(03)00137-7

8. Roberg-Larsen H, Strand MF, Krauss S, Wilson SR. Metabolites in vertebrate hedgehog signaling. *Biochem Biophys Res Commun* (2014) 446:669–74. doi: 10.1016/j.bbrc.2014.01.087

9. Gustafsson JA, Eneroth P. Steroids in meconium and faeces from newborn infants. *Proc R Soc Lond B Biol Sci* (1972) 180:179–86. doi: 10.1098/rspb.1972.0013

10. Eneroth P, Gustafsson J. Steroids in newborns and infants. hydroxylated cholesterol derivatives in the steroid monosulphate fraction from meconium. *FEBS Lett* (1969) 3:129–32. doi: 10.1016/0014-5793(69)80115-8

11. Crick PJ, William Bentley T, Abdel-Khalik J, Matthews I, Clayton PT, Morris AA, et al. Quantitative charge-tags for sterol and oxysterol analysis. *Clin Chem* (2015) 61:400–11. doi: 10.1373/clinchem.2014.231332

12. Raselli T, Hearn T, Wyss A, Atrott K, Peter A, Frey-Wagner I, et al. Elevated oxysterol levels in human and mouse livers reflect nonalcoholic steatohepatitis. *J Lipid Res* (2019) 60:1270–83. doi: 10.1194/jlr.M093229

13. Griffiths WJ, Crick PJ, Meljon A, Theofilopoulos S, Abdel-Khalik J, Yutuc E, et al. Additional pathways of sterol metabolism: Evidence from analysis of Cyp27a1-/- mouse brain and plasma. *Biochim Biophys Acta Mol Cell Biol Lipids* (2019) 1864:191–211. doi: 10.1016/j.bbalip.2018.11.006

14. Abdel-Khalik J, Yutuc E, Crick PJ, Gustafsson JA, Warner M, Roman G, et al. Defective cholesterol metabolism in amyotrophic lateral sclerosis. *J Lipid Res* (2017) 58:267–78. doi: 10.1194/jlr.P071639

15. Phinney KW, Ballihaut G, Bedner M, Benford BS, Camara JE, Christopher SJ, et al. Development of a standard reference material for metabolomics research. *Anal Chem* (2013) 85:11732–8. doi: 10.1021/ac402689t

16. Quehenberger O, Armando AM, Brown AH, Milne SB, Myers DS, Merrill AH, et al. Lipidomics reveals a remarkable diversity of lipids in human plasma. *J Lipid Res* (2010) 51:3299–305. doi: 10.1194/jlr.M009449

17. Chung BC, Matteson KJ, Voutilainen R, Mohandas TK, Miller WL. Human cholesterol side-chain cleavage enzyme, P450scc: cDNA cloning, assignment of the gene to chromosome 15, and expression in the placenta. *Proc Natl Acad Sci U.S.A.* (1986) 83:8962–6. doi: 10.1073/pnas.83.23.8962

18. Griffiths WJ, Hearn T, Crick PJ, Abdel-Khalik J, Dickson A, Yutuc E, et al. Charge-tagging liquid chromatography-mass spectrometry methodology targeting oxysterol diastereoisomers. *Chem Phys Lipids* (2017) 207:69–80. doi: 10.1016/j.chemphyslip.2017.04.004

19. Yutuc E, Dickson AL, Pacciarini M, Griffiths L, Baker PRS, Connell L, et al. Deep mining of oxysterols and cholestenoic acids in human plasma and cerebrospinal fluid: Quantification using isotope dilution mass spectrometry. *Anal Chim Acta* (2021) 1154:338259. doi: 10.1016/j.aca.2021.338259

20. Sidhu R, Jiang H, Farhat NY, Carrillo-Carrasco N, Woolery M, Ottinger E, et al. A validated LC-MS/MS assay for quantification of 24(S)-hydroxycholesterol in plasma and cerebrospinal fluid. *J Lipid Res* (2015) 56:1222–33. doi: 10.1194/jlr.D058487

21. Stiles AR, Kozlitina J, Thompson BM, McDonald JG, King KS, Russell DW. Genetic, anatomic, and clinical determinants of human serum sterol and vitamin d levels. *Proc Natl Acad Sci U.S.A.* (2014) 111:E4006–4014. doi: 10.1073/pnas.1413561111

22. Griffiths WJ, Yutuc E, Abdel-Khalik J, Crick PJ, Hearn T, Dickson A, et al. Metabolism of non-enzymatically derived oxysterols: Clues from sterol metabolic disorders. *Free Radic Biol Med* (2019) 144:124–33. doi: 10.1016/j.freeradbiomed.2019.04.020

23. Dickson A, Yutuc E, Thornton CA, Dunford JE, Oppermann U, Wang Y, et al. HSD3B1 is an oxysterol 3β-hydroxysteroid dehydrogenase in human placenta. *bioRxiv* (2022) 2004.2001:486576. doi: 10.1101/2022.04.01.486576

24. Cali JJ, Russell DW. Characterization of human sterol 27-hydroxylase. A mitochondrial cytochrome p-450 that catalyzes multiple oxidation reaction in bile acid biosynthesis. *J Biol Chem* (1991) 266:7774–8. doi: 10.1016/S0021-9258(20)89517-9

25. Uhlen M, Fagerberg L, Hallstrom BM, Lindskog C, Oksvold P, Mardinoglu A, et al. Proteomics. tissue-based map of the human proteome. *Science* (2015) 347:1260419. doi: 10.1126/science.1260419

26. Axelson M, Sjovall J. Potential bile acid precursors in plasma–possible indicators of biosynthetic pathways to cholic and chenodeoxycholic acids in man. *J Steroid Biochem* (1990) 36:631–40. doi: 10.1016/0022-4731(90)90182-R

27. Russell DW. The enzymes, regulation, and genetics of bile acid synthesis. *Annu Rev Biochem* (2003) 72:137–74. doi: 10.1146/annurev.biochem.72.121801.161712

28. Griffiths WJ, Wang Y. Oxysterols as lipid mediators: Their biosynthetic genes, enzymes and metabolites. *Prostaglandins Other Lipid Mediat* (2020) 147:106381. doi: 10.1016/j.prostaglandins.2019.106381

29. Yutuc E, Angelini R, Baumert M, Mast N, Pikuleva I, Newton J, et al. Localization of sterols and oxysterols in mouse brain reveals distinct spatial cholesterol metabolism. *Proc Natl Acad Sci U.S.A.* (2020) 117:5749–60. doi: 10.1073/pnas.1917421117

30. Schroepfer GJJr. Oxysterols: modulators of cholesterol metabolism and other processes. *Physiol Rev* (2000) 80:361–554. doi: 10.1152/physrev.2000.80.1.361

31. Lehmann JM, Kliewer SA, Moore LB, Smith-Oliver TA, Oliver BB, Su JL, et al. Activation of the nuclear receptor LXR by oxysterols defines a new hormone response pathway. *J Biol Chem* (1997) 272:3137–40. doi: 10.1074/jbc.272.6.3137

32. Jin L, Martynowski D, Zheng S, Wada T, Xie W, Li Y. Structural basis for hydroxycholesterols as natural ligands of orphan nuclear receptor RORgamma. *Mol Endocrinol* (2010) 24:923–9. doi: 10.1210/me.2009-0507

33. Nachtergaele S, Mydock LK, Krishnan K, Rammohan J, Schlesinger PH, Covey DF, et al. Oxysterols are allosteric activators of the oncoprotein smoothened. *Nat Chem Biol* (2012) 8:211–20. doi: 10.1038/nchembio.765

34. Nachtergaele S, Whalen DM, Mydock LK, Zhao Z, Malinauskas T, Krishnan K, et al. Structure and function of the smoothened extracellular domain in vertebrate hedgehog signaling. *Elife* (2013) 2:e01340. doi: 10.7554/eLife.01340

35. Goldstein JL, DeBose-Boyd RA, Brown MS. Protein sensors for membrane sterols. *Cell* (2006) 124:35–46. doi: 10.1016/j.cell.2005.12.022

36. Abrams ME, Johnson KA, Perelman SS, Zhang LS, Endapally S, Mar KB, et al. Oxysterols provide innate immunity to bacterial infection by mobilizing cell surface accessible cholesterol. *Nat Microbiol* (2020) 5:929–42. doi: 10.1038/s41564-020-0701-5

37. Radhakrishnan A, Ikeda Y, Kwon HJ, Brown MS, Goldstein JL. Sterol-regulated transport of SREBPs from endoplasmic reticulum to golgi: oxysterols block transport by binding to insig. *Proc Natl Acad Sci U.S.A.* (2007) 104:6511–8. doi: 10.1073/pnas.0700899104

38. Cheng Y-S, Zhang T, Ma X, Pratuangtham S, Zhang GC, Ondrus AA, et al. A proteome-wide map of 20(S)-hydroxycholesterol interactors in cell membranes. *Nat Chem Biol* (2021) 17:1271–80. doi: 10.1038/s41589-021-00907-2

39. Yu W, Baskin JM. There is a lock for every key. *Nat Chem Biol* (2021) 17:1214–6. doi: 10.1038/s41589-021-00908-1

40. Guryev O, Carvalho RA, Usanov S, Gilep A, Estabrook RW. A pathway for the metabolism of vitamin D3: Unique hydroxylated metabolites formed during catalysis with cytochrome P450scc (CYP11A1). *Proc Natl Acad Sci* (2003) 100:14754–9. doi: 10.1073/pnas.2336107100

41. Tuckey RC, Li W, Zjawiony JK, Zmijewski MA, Nguyen MN, Sweatman T, et al. Pathways and products for the metabolism of vitamin D3 by cytochrome P450scc. *FEBS J* (2008) 275:2585–96. doi: 10.1111/j.1742-4658.2008.06406.x

42. Roberg-Larsen H, Strand MF, Grimsmo A, Olsen PA, Dembinski JL, Rise F, et al. High sensitivity measurements of active oxysterols with automated filtration/filter backflush-solid phase extraction-liquid chromatography-mass spectrometry. *J Chromatogr A* (2012) 1255:291–7. doi: 10.1016/j.chroma.2012.02.002

43. Spencer TA, Li D, Russel JS, Collins JL, Bledsoe RK, Consler TG, et al. Pharmacophore analysis of the nuclear oxysterol receptor LXRα. *J Medicinal Chem* (2001) 44:886–97. doi: 10.1021/jm0004749

44. Tranheim Kase E, Andersen B, Nebb HI, Rustan AC, Hege Thoresen G. 22-hydroxycholesterols regulate lipid metabolism differently than T0901317 in human myotubes. *Biochim Biophys Acta (BBA) - Mol Cell Biol Lipids* (2006) 1761:1515–22. doi: 10.1016/j.bbalip.2006.09.010

45. Forman BM, Ruan B, Chen J, Schroepfer GJ, Evans RM. The orphan nuclear receptor LXRα is positively and negatively regulated by distinct products of mevalonate metabolism. *Proc Natl Acad Sci* (1997) 94:10588–93. doi: 10.1073/pnas.94.20.10588

46. Korach-André M, Gustafsson J. Liver X receptors as regulators of metabolism. *Biomol Concepts* (2015) 6:177–90. doi: 10.1515/bmc-2015-0007

47. Sacchetti P, Sousa KM, Hall AC, Liste I, Steffensen KR, Theofilopoulos S, et al. Liver X receptors and oxysterols promote ventral midbrain neurogenesis *in vivo* and in human embryonic stem cells. *Cell Stem Cell* (2009) 5:409–19. doi: 10.1016/j.stem.2009.08.019

48. Dai Y-b, Tan X-j, Wu W-f, Warner M, Gustafsson. J.-Å. Liver X receptor β protects dopaminergic neurons in a mouse model of Parkinson disease. *Proc Natl Acad Sci* (2012) 109:13112–7. doi: 10.1073/pnas.1210833109

49. Tuckey RC, Cameron KJ. Side-chain specificities of human and bovine cytochromes p-450scc. *Eur J Biochem* (1993) 217:209–15. doi: 10.1111/j.1432-1033.1993.tb18235.x

50. Thomas JL, Myers RP, Strickler RC. Human placental 3 beta-hydroxy-5-ene-steroid dehydrogenase and steroid 5--4-ene-isomerase: purification from mitochondria and kinetic profiles, biophysical characterization of the purified mitochondrial and microsomal enzymes. *J Steroid Biochem* (1989) 33:209–17. doi: 10.1016/0022-4731(89)90296-3

51. Chapman JC, Polanco JR, Min S, Michael SD. Mitochondrial 3 beta-hydroxysteroid dehydrogenase (HSD) is essential for the synthesis of progesterone by corpora lutea: An hypothesis. *Reprod Biol Endocrinol* (2005) 3:11. doi: 10.1186/1477-7827-3-11

52. Simard J, Ricketts ML, Gingras S, Soucy P, Feltus FA, Melner MH. Molecular biology of the 3beta-hydroxysteroid dehydrogenase/delta5-delta4 isomerase gene family. *Endocr Rev* (2005) 26:525–82. doi: 10.1210/er.2002-0050

53. Astle S, Slater DM, Thornton S. The involvement of progesterone in the onset of human labour. *Eur J Obstet Gynecol Reprod Biol* (2003) 108:177–81. doi: 10.1016/S0301-2115(02)00422-0

54. Nadeem L, Shynlova O, Matysiak-Zablocki E, Mesiano S, Dong X, Lye S. Molecular evidence of functional progesterone withdrawal in human myometrium. *Nat Commun* (2016) 7:11565. doi: 10.1038/ncomms11565

55. Une M, Tsujimura K, Kihira K, Hoshita T. Identification of (22R)-3 alpha,7 alpha,12 alpha,22- and (23R)-3 alpha,7 alpha,12 alpha,23-tetrahydroxy-5 beta-cholestanoic acids in urine from a patient with zellweger's syndrome. *J Lipid Res* (1989) 30:541–7. doi: 10.1016/S0022-2275(20)38346-2

56. Lambeth JD, Kitchen SE, Farooqui AA, Tuckey R, Kamin H. Cytochrome p-450scc-substrate interactions. studies of binding and catalytic activity using hydroxycholesterols. *J Biol Chem* (1982) 257:1876–84. doi: 10.1016/S0021-9258(19)68119-6

57. Bartz F, Kern L, Erz D, Zhu M, Gilbert D, Meinhof T, et al. Identification of cholesterol-regulating genes by targeted RNAi screening. *Cell Metab* (2009) 10:63–75. doi: 10.1016/j.cmet.2009.05.009